NASA Technical Memorandum 87746

NASA-TM-87746 19860020161

INTERACTION OF AIRBORNE AND STRUCTUREBORNE NOISE RADIATED BY PLATES VOLUME I -- ANALTYICAL STUDY

MICHAEL C. McGARY

JULY 1986

NASA
National Aeronautics and Space Administration

Langley Research Center
Hampton, Virginia 23665

SUMMARY

An analytical study was undertaken in order to further the understanding of the interaction of airborne and structureborne noise radiated by aircraft materials. The theory and the results of several computer simulations of the noise radiated by thin, isotropic, rectangular aluminum plates due to fully coherent combined acoustic and vibrational inputs is presented. The most significant finding of the study was the extremely large influence that the relative phase between the inputs has on the combined noise radiation of the plates. It is shown that phase dependent effects manifest themselves as cross terms in both the dynamic and acoustic portions of the analysis. The computer simulations show that these cross terms can radically alter the combined sound power radiated by plates constructed of aircraft-type materials. The results of the study suggest that airborne-structureborne interactive effects could be responsible for a significant portion of the overall noise radiated by aircraft-type structures in the low frequency regime. This implies that previous analytical and experimental studies may have neglected an important physical phenomenon in their analyses of the interior noise of propeller driven aircraft.

LIST OF SYMBOLS

a_{kl}	influence coefficient of the klth structural mode due to an acoustic (airborne) input
a_{mn}	influence coefficient of the mnth structural mode due to an acoustic (airborne) input
c_o	speed of sound in air at ambient atmospheric conditions
c_1	location of the point vibrational input in the α_1 coordinate direction
c_2	location of the point vibrational input in the α_2 coordinate direction
d_1	plate dimension in the α_1 coordinate direction
d_2	plate dimension in the α_2 coordinate direction
D_{ij}	flexural rigidity which relates bending moments to the curvature of the plate (i,j=1,2,6)
$\vec{e}_r$,$\vec{e}_{r'}$	radially outward unit vectors
E	modulus of elasticity (Young's modulus)
f	frequency, Hertz
f_a	airborne forcing function (acoustic input)
f_s	structureborne forcing function (vibrational input)
G	shear modulus of elasticity (modulus of rigidity)
h	thickness of the plate - also used as the distance between a monopole and a nearby reflecting surface
I	magnitude of the acoustic intensity vector
$\vec{I}$	acoustic intensity vector
j	square root of -1 (imaginary number)

LIST OF SYMBOLS (cont'd)

k	alternate mode number for the α_1 coordinate
l	alternate mode number for the α_2 coordinate
m	mode number for the α_1 coordinate
n	mode number for the α_2 coordinate
$\vec{n}$	unit vector normal to the surface
p	acoustic pressure
q	forcing function applied to the plate
r	distance between the origin of the coordinate system and the point of observation
$\vec{r}$	position vector of the point of observation
r'	distance between an arbitrary point on the plate and the point of observation
$\vec{r}'$	vector joining an acoustic monopole radiator and the point of observation
r_1, r_2, r_3	coordinates of the point of observation
Re{ }	real part of the quantity inside brackets
S	surface area of the plate (one side)
s_{kl}	influence coefficient of the klth structural mode of the plate due to a vibrational (structureborne) input
s_{mn}	influence coefficient of the mnth structural mode of the plate due to a vibrational (structureborne) input
t	time
u	transverse displacement of the plate
$\dot{u}$	transverse velocity of the plate

v	magnitude of the acoustic fluid particle velocity vector - often used interchangeably with the transverse velocity of the plate since the two quantities are equal at the surface of the plate
$\vec{v}$	acoustic fluid particle velocity vector
$\dot{W}$	power input to the plate by the forcing function
Z_k	complex number associated with the kth mode (the result of evaluating a Raleigh integral)
Z_l	complex number associated with the lth mode (the result of evaluating a Raleigh integral)
Z_m	complex number associated with the mth mode (the result of evaluating a Raleigh integral)
Z_n	complex number associated with the nth mode (the result of evaluating a Raleigh integral)

Greek

$\alpha_1, \alpha_2, \alpha_3$	cartesian coordinate system with the origin at the corner of the plate
$\beta_1, \beta_2, \beta_3$	cartesian coordinate system with the origin at the center of the plate
γ	dummy complex argument
γ_{kl}	phase angle associated with the klth mode due to the damping coefficient ξ_{kl}
γ_{mn}	phase angle associated with the mnth mode due to the damping coefficient ξ_{mn}
δ	Dirac delta function
η_i	modal participation factor for the ith mode
η_{kl}	influence coefficient of the klth mode
η_{mn}	influence coefficient of the mnth mode
θ	polar angle in a spherical coordinate system

Greek (cont'd)

Θ_{kl}	phase angle associated with the klth mode
Θ_{mn}	phase angle associated with the mnth mode
λ	equivalent viscous damping coefficient
μ	Poisson's ratio for an isotropic material
ξ_{mn}	equivalent viscous critical damping coefficient associated with the mnth mode
Π	sound power radiated by the plate
ρ	mass per unit area of the plate
ρ_o	density of the acoustic fluid medium (air)
ϕ	azimuthal angle in spherical coordinates
ϕ_a	relative phase of the airborne input
ϕ_s	relative phase of the structureborne input
ω	radian frequency of the forcing function
ω_{mn}	radian natural frequency of the mnth mode
Ω_{mn}	damped radian modal natural frequency

Superscripts

*	denotes the complex conjugate
$\rightarrow$	denotes a vector

Special symbols

$< >_t$	denotes a time average
$< >_{r,t}$	denotes a space-time average
$\| \|$	denotes the magnitude of the quantity inside

1. INTRODUCTION

High interior noise levels in propeller driven aircraft have historically been a cause for concern in both the commercial and military sectors of the aircraft industry. Future problems with interior noise levels in aircraft are expected to intensify due to the advanced turboprop propulsion systems now being incorporated into the design of transport aircraft.

The noise entering the cabin of a propeller driven aircraft is generally divided into two major categories, viz. airborne noise and structureborne noise. Airborne noise is generated aerodynamically by the propellers, propagates along an acoustic path, and is transmitted through the sidewalls of the aircraft into the interior. Structureborne noise has its source in the vibration of the wings or other structural members of the aircraft. This vibrational energy propagates along structural paths into the aircraft where it causes vibration of the various surfaces in the cabin and ultimately radiates noise.

The distinction between airborne and structureborne noise is important because the methods typically used in reducing airborne and structureborne noise are quite different. For example, if the predominant source of the noise in the aircraft is structureborne, then the problem might be solved through the use of vibration isolators, or by the

application of damping materials. If the predominant source of the noise is airborne, then the problem might be solved by aft mounting the propellers or by adding massive materials to the sidewalls.

Because of the different treatment methods for the airborne and structureborne components of the noise, researchers, in the past, have devoted their attention almost exclusively to either the airborne path or the structureborne path. (See reference [1] for a summary of past research on the airborne path and references [2]-[4] for some of the more recent efforts aimed at structureborne noise.) While this separatist approach may produce more efficient methods for treatment of the two individual paths, it neglects the possible interaction that may take place between the airborne and structureborne components. An interactive component arises due to the coherent nature of the noise propagated along these two paths. (The airborne and structureborne noises are fully coherent since they both have the same source, viz. the propellers.) Presently, the relative importance of these interactive effects in propeller driven aircraft is unknown. The purpose of this paper is to present the theoretical developments of a study [5] which was aimed at furthering the understanding of the interaction between the airborne and structureborne noise. In addition to the theory, the results of several computer

simulations are presented for the noise radiated by aircraft type materials due to fully coherent combined acoustic and vibrational inputs in the low frequency regime.

2. PROBLEM APPROACH

In order to fully understand the interaction between airborne and structureborne noise, both analytical and experimental studies were performed. The analytical model was used to simulate the noise radiation of a structure due to simultaneously combined coherent acoustic and vibrational inputs. The experimental study was then used to verify the behavior predicted by the analytical model. This paper presents the details of the analytical model and the results of the computer simulations. The apparatus used for the experimental study and the results obtained from the experiments will be presented in another paper.

Simple isotropic rectangular plates served as the test vehicle for the studies. Plates were chosen because they possess most of the vibrational and sound radiative properties that are exhibited by actual aircraft sidewalls (due to their thin shell construction). The analytical model assumes that the plates are rectangular and simply supported in an infinite, rigid baffle. The sound radiated by the plates is assumed to be generated by the flexural (bending) vibrational response of the plate and is radiated to a free-field acoustic space (anechoic). Futhermore, the dynamic

response of the plate (which generates the sound) is assumed to be dependent only on the incident airborne and structure-borne forcing functions on the plate and independent of (uncoupled from) the sound pressure radiated by the plate. The plate geometry is defined in figure (1).

A normally incident, spatially uniform pressure field was used to model the airborne input. A point load was used to model the structureborne input. The analysis was confined to the 0-1000 Hz frequency range since this range encompasses the most troublesome noise region for propeller driven aircraft.

The effects of several parameters on the interaction between the airborne and structureborne components were investigated. Parameters studied included the relative magnitude and phase of the acoustic and vibrational inputs, the location of the structureborne input, and the level of structural damping.

3. ANALYSIS OF THE DYNAMIC RESPONSE

3.1 FREE VIBRATIONAL RESPONSE FOR THE UNDAMPED CASE

The governing differential equation for the free dynamic response of an undamped, simply supported, rectangular orthotropic plate (from reference [6]) is given by

$$D_{11}\partial^4 u/\partial\alpha_1^4 + 2(D_{12}+2D_{66})\partial^4 u/\partial\alpha_1^2\partial\alpha_2^2 + D_{22}\partial^4 u/\partial\alpha_2^4 + \rho h\ddot{u} = 0 , \qquad (1)$$

where the plate rigidity constants that relate the internal bending and twisting moments of the plate to the twists and curvatures they induce are given by

$$D_{11} = h^3/12\ E_1/(1-\mu_1\mu_2)\ , \tag{2}$$

$$D_{22} = h^3/12\ E_2/(1-\mu_1\mu_2)\ , \tag{3}$$

$$D_{12} = h^3/12\ E_1\mu_2/(1-\mu_1\mu_2) = h^3/12\ E_2\mu_1/(1-\mu_1\mu_2)\ , \tag{4}$$

$$D_{66} = h^3/12\ G\ , \tag{5}$$

where

E_i = the effective modulus of elasticity (Young's modulus) in the ith direction,

μ_i = the effective Poisson's ratio in the ith direction,

G = the shear modulus of elasticity (modulus of rigidity),

h = is the thickness of the plate.

If the plate is simply supported on all four edges, the boundary conditions are zero displacement and zero bending moment along the edges. It can be shown that these two boundary conditions can be expressed as (see reference [6])

at $\alpha_1 = 0, d_1$

$u = 0$, and (6)

$$D_{11}\partial^2 u/\partial\alpha_1^2 + D_{12}\partial^2 u/\partial\alpha_2^2 = 0 , \quad (7)$$

and at $\alpha_2 = 0, d_2$

$u = 0$, and (8)

$$D_{12}\partial^2 u/\partial\alpha_1^2 + D_{22}\partial^2 u/\partial\alpha_2^2 = 0 . \quad (9)$$

The general solution of the homogeneous partial differential equation is given by a series expansion in the natural modes of the structure:

$$u(\alpha_1, \alpha_2, t) =$$

$$\sum_{m=1}^{\infty} \sum_{n=1}^{\infty} \eta_{mn} \sin(m\pi\alpha_1/d_1) \sin(n\pi\alpha_2/d_2) e^{j(\omega_{mn}t + \theta_{mn})} . \quad (10)$$

where

η_{mn} = the influence coefficients of the modes in units of displacement,

ω_{mn} = the radian natural frequencies of the modes, and

θ_{mn} = the phase angles associated with the modes.

It is easily shown that this solution satisfies all of the simple support boundary conditions. Substituting this solution into the governing partial differential equation of motion it can easily be shown that the radian natural frequencies are given by the relation

$$\omega_{mn}^2 = \pi^4/\rho h \cdot \left[D_{11}(m/d_1)^4 + 2(D_{12}+2D_{66})(m/d_1)^2(n/d_2)^2 + D_{22}(n/d_2)^4 \right] . \quad (11)$$

3.2 FREE VIBRATIONAL RESPONSE OF THE DAMPED CASE

Including an equivalent viscous damping term, the governing equation becomes

$$D_{11}\partial^4 u/\partial\alpha_1^4 + 2(D_{12}+2D_{66})\partial^4 u/\partial\alpha_1^2\partial\alpha_2^2 + D_{22}\partial^4 u/\partial\alpha_2^4 + \lambda\dot{u} + \rho h\ddot{u} = 0 . \quad (12)$$

By assuming that the vibrational modes of the plate are uncoupled, the modal damping coefficient can be defined as

$$\xi_{mn} = \lambda/(2\rho h\omega_{mn}) . \quad (13)$$

Technically, the flexural modeshapes of a rectangular plate are uncoupled only when the damping is linearly related to the mass and stiffness properties of the plate in a special fashion. Thus, by making this assumption, our mathematical relations for the orthotropic plate become approximations.

The assumption that the modes are uncoupled can be used without serious error when the damping is a second order effect. Furthermore, the assumption is aided by the fact that the modal density for flexural modes of a rectangular plate is nearly constant at low frequency. This means that there are no frequency regions of high modal density and therefore little opportunity for the exchange of vibrational energy among modes.

Substituting into the governing equation, one obtains

$$D_{11}\partial^4 u/\partial\alpha_1^4 + 2(D_{12}+2D_{66})\partial^4 u/\partial\alpha_1^2\partial\alpha_2^2 + D_{22}\partial^4 u/\partial\alpha_2^4$$

$$+\rho h 2\xi_{mn}\omega_{mn}\dot{u} + \rho h\ddot{u} = 0 \ . \qquad (14)$$

Assuming a solution of the form

$$u(\alpha_1,\alpha_2,t) =$$

$$\sum_{m=1}^{\infty}\sum_{n=1}^{\infty} \eta_{mn}\sin(m\pi\alpha_1/d_1)\sin(n\pi\alpha_2/d_2)\, e^{\gamma t+j\theta_{mn}} \ , \qquad (15)$$

and substituting back into the governing equation, it can shown that the general solution to the damped free vibration problem is

$$u(\alpha_1,\alpha_2,t) =$$

$$\sum_{m=1}^{\infty}\sum_{n=1}^{\infty} \eta_{mn}\sin(m\pi\alpha_1/d_1)\sin(n\pi\alpha_2/d_2)$$

$$\cdot\, e^{-\xi_{mn}\omega_{mn}t}\, e^{j(\Omega_{mn}t+\theta_{mn})} \,. \qquad (16)$$

where the damped radian natural frequencies are defined by

$$\Omega_{mn} = \omega_{mn}\left[\, 1-\xi_{mn}^2 \,\right]^{1/2} \,. \qquad (17)$$

Damping coefficients of the form given by equation (13) do not always accurately model the physical behavior exhibited by a plate. At higher frequencies the damping coefficients of 2024 aluminum are relatively independent of frequency and are in the range of $\xi = 0.01$. A more moderately damped structure might have damping coefficients in the range $\xi = 0.04$. Because of the large energy loss due to sound radiation at low frequency, however, experimentally determined damping coefficients for the first few resonance frequencies will appear to be much, much larger than this. (On the order of $\xi = 0.1$.) These inflated damping coefficients at low resonance frequencies are the result of neglecting the significant fluid loading effect in the model of the forcing function. For these reasons, two different damping models were investigated in this study given by the equations

$$\xi_{mn} = .09(\omega_{11}/\omega_{mn}) + .01 \ , \tag{18}$$

$$\xi_{mn} = .06(\omega_{11}/\omega_{mn}) + .04 \ , \tag{19}$$

where the hyberbolic term in each equation corrects for the fluid loading effect at the first few resonance frequencies and the constant term in each equation represents the inherent damping of the structure. Equation (18) shall be subsequently referred to as the small damping model while equation (19) shall be referred to as the moderate damping model.

3.3 FORCED VIBRATIONAL RESPONSE

The general forced vibrational response of a simply supported, rectangular orthotropic plate is governed by the non-homogeneous partial differential equation

$$D_{11}\partial^4 u/\partial\alpha_1^4 + 2(D_{12} + 2D_{66})\partial^4 u/\partial\alpha_1^2\partial\alpha_2^2 + D_{22}\partial^4 u/\partial\alpha_2^4$$

$$+ \lambda\dot{u} + \rho h\ddot{u} = q(\alpha_1,\alpha_2,t) \ , \tag{20}$$

where, for the purposes of this study, the forcing function $q(\alpha_1,\alpha_2,t)$ will be defined by the equation

$$q(\alpha_1,\alpha_2,t) =$$

$$\left[f_s \, e^{-j\phi_s} \, \delta(\alpha_1-c_1)\delta(\alpha_2-c_2) + f_a \, e^{-j\phi_a} \right] e^{j\omega t} \ . \tag{21}$$

The various parameters in equation (21) are

f_s = the magnitude of the structureborne input (units of force),

ϕ_s = the relative phase of the structureborne input,

f_a = the magnitude of the airborne input (units of force/area),

ϕ_a = the relative phase of the airborne input,

c_1 = the location of the point vibrational input in the α_1 coordinate direction,

c_2 = the location of the point vibrational input in the α_1 coordinate direction,

ω = the radian frequency of the simple harmonic forcing function,

and the symbol δ denotes the dirac delta function. Thus, the acoustic (airborne) input is chosen to be a normally incident, spatially uniform, simple harmonic forcing function and the vibrational (structureborne) input is chosen to be a simple harmonic, point vibrational load.

The reasons for choosing a normally incident airborne input are twofold. First of all, the propeller noise which impinges on the sidewall of an aircraft defines an oblique incidence problem. The spatial pressure distribution of this incident sound is slowly varying due to the extremely long wavelengths of the low frequency sound. Therefore,

over small regions of the aircraft sidewalls, the spatial distribution of the pressure is nearly uniform. Secondly, it is comparatively much easier to construct an experimental apparatus that approximates the normal incidence condition.

The point vibrational input was chosen to model the structureborne input primarily because it emulates the type of forcing function obtained experimentally using a shaker. It might be argued that a line load is a more realistic structureborne model since aircraft panels have ring frames and stringers attached to them. Because of the wide variation in design of airframes and in wing attachment, however, it is not clear that a line load model would be any more realistic. Furthermore, for the purposes of understanding the interactive effects of the airborne and structureborne components, the point load model will, in principle, work just as well as a more complicated model.

The forcing function of equation (21) can be expanded into a series representation using the eigenfunctions of the plate as follows:

$$q(\alpha_1,\alpha_2,t) =$$

$$\left[\sum_{m=1}^{\infty} \sum_{n=1}^{\infty} q_{mn} \sin(m\pi\alpha_1/d_1)\sin(n\pi\alpha_2/d_2) \right] e^{j\omega t} . \qquad (22)$$

Utilizing the orthogonality principle it can be shown that the coefficients q_{mn} are given by

$$q_{mn} = 4f_s\, e^{-j\phi_s}/(d_1 d_2)\, \sin(m\pi c_1/d_1)\sin(n\pi c_2/d_2)$$

$$+\ 4f_a\, e^{-j\phi_a}/(mn\pi^2)\,(1-\cos(m\pi))(1-\cos(n\pi))\ . \qquad (23)$$

The solution to equation (20) is of the form

$$u(\alpha_1,\alpha_2,t) =$$

$$\sum_{m=1}^{\infty}\sum_{n=1}^{\infty} \eta_{mn}\sin(m\pi\alpha_1/d_1)\sin(n\pi\alpha_2/d_2)\, e^{j(\omega t-\theta_{mn})}\ . \qquad (24)$$

where the transient (complementary) solution has been neglected, since it exponentially decays to zero, and only the steady state (particular) solution is considered. Substituting (24) into the governing equation (20) and equating the coefficients of the resultant series,

$$\left[\ \rho h\omega_{mn}^2+\rho h 2\xi_{mn}\omega_{mn}(j\omega)-\rho h\omega^2\ \right]\ \eta_{mn}\, e^{-j\theta_{mn}} =$$

$$4f_s\, e^{-j\phi_s}/(d_1 d_2)\, \sin(m\pi c_1/d_1)\sin(n\pi c_2/d_2)$$

$$+\ 4f_a\, e^{-j\phi_a}/(mn\pi^2)\,(1-\cos(m\pi))(1-\cos(n\pi))\ . \qquad (25)$$

Utilizing the theory of complex variables, the term in brackets on the left side of equation (25) is given by

$$\left[\rho h\omega_{mn}^2 + \rho h 2\xi_{mn}(j\omega) - \rho h\omega^2 \right] =$$

$$\rho h\omega_{mn}^2 \left[(1-\omega^2/\omega_{mn}^2)^2 + (2\xi_{mn}\omega/\omega_{mn})^2 \right]^{1/2} e^{j\gamma_{mn}} , \qquad (26)$$

where the phase angle γ_{mn} is defined to be

$$\gamma_{mn} = \tan^{-1} \left[(2\xi_{mn}\omega/\omega_{mn})/(1-\omega^2/\omega_{mn}^2) \right] . \qquad (27)$$

Dividing equation (25) by equation (26) yields the modal participation factors

$$\eta_{mn} e^{-j\theta_{mn}} = \left[s_{mn} e^{-j\phi_s} + a_{mn} e^{-j\phi_a} \right] e^{-j\gamma_{mn}} , \qquad (28)$$

where the modal influence coefficients are seen to be

$$s_{mn} = 4f_s/(d_1 d_2 \rho h\omega_{mn}^2) \sin(m\pi c_1/d_1)\sin(n\pi c_2/d_2)$$

$$/ \left[(1-\omega^2/\omega_{mn}^2)^2 + (2\xi_{mn}\omega/\omega_{mn})^2 \right]^{1/2} , \qquad (29)$$

and

$$a_{mn} = 4f_a/(mn\pi^2 \rho h\omega_{mn}^2) \left[(1-\cos(m\pi))(1-\cos(n\pi)) \right]$$

$$/ \left[(1-\omega^2/\omega_{mn}^2)^2 + (2\xi_{mn}\omega/\omega_{mn})^2 \right]^{1/2} . \qquad (30)$$

Thus, the steady state solution for the plate transverse displacement is

$$u(\alpha_1,\alpha_2,t) = \sum_{m=1}^{\infty} \sum_{n=1}^{\infty} \left[s_{mn}\, e^{-j\phi_s} + a_{mn}\, e^{-j\phi_a} \right]$$

$$\cdot \sin(m\pi\alpha_1/d_1)\sin(n\pi\alpha_2/d_2)\, e^{j(\omega t-\gamma_{mn})} . \qquad (31)$$

Simple differentiation with respect to time leads to an equation for the vibrational velocity of the plate given by:

$$v(\alpha_1,\alpha_2,t) =$$

$$\sum_{m=1}^{\infty} \sum_{n=1}^{\infty} \left[j\omega \left[s_{mn}\, e^{-j\phi_s} + a_{mn}\, e^{-j\phi_a} \right] \right.$$

$$\left. \cdot \sin(m\pi\alpha_1/d_1)\sin(n\pi\alpha_2/d_2)\, e^{j(\omega t-\gamma_{mn})} \right] . \qquad (32)$$

3.4 POWER DISSIPATED BY THE PLATE

It can be shown that the time averaged power dissipated by the plate (see references [5] or [6]) is given by

$$\langle \dot{W}(t) \rangle_t =$$

$$\lambda \int_0^{d_2} \int_0^{d_1} 1/2 \; \mathrm{Re}\{v^*(\vec{r},t) v(\vec{r},t)\} \; d\alpha_1 d\alpha_2$$

$$= \lambda \int_0^{d_2} \int_0^{d_1} \langle v^2(\vec{r},t) \rangle_t \; d\alpha_1 d\alpha_2 = \lambda S \langle v^2(\vec{r},t) \rangle_{r,t} \; . \qquad (33)$$

After lengthy complex algebra and straightforward integration, substitution of equation (32) into equation (33) leads to the result

$$\langle \dot{W}(t) \rangle_t = \omega^2/8 \cdot$$

$$\sum_{m=1}^{\infty} \sum_{n=1}^{\infty} \lambda S \left[s_{mn}^2 + a_{mn}^2 + 2 s_{mn} a_{mn} \cos(\phi_s - \phi_a) \right]. \qquad (34)$$

The last term in equation (34) accounts for the interaction between the structureborne and airborne inputs in terms of the panel dynamics. Thus, equation (34) shows that the dynamic response of the panel to the combined airborne and structureborne inputs is, in general, not equal to the sum of the responses to the airborne and structureborne inputs

individually. Similar cross term components arise in the derivations of the power input to the plate. (See reference [5].) One of the important features of equation (34) is that although it contains cross terms due to the combined inputs, it contains no cross terms between different modes of the structure. This absence of cross terms between modes is a direct consequence of the orthogonality principle between modes of the structure. Equation (34) indicates that when the structureborne and the airborne inputs are precisely 90 degrees out of phase, the inputs are uncorrelated and the cross term is zero. Thus, when the two inputs are uncorrelated, the power dissipated by the panel due to the combined inputs is exactly equal to the sum of the powers dissipated due to the structureborne and airborne inputs acting individually.

4. ANALYSIS OF THE ACOUSTIC RESPONSE

Once the surface velocity distribution of the plate has been found (equation (32)), the sound generated by the plate can be calculated. The classical approach for calculating the sound power radiated from a vibrating plate, which utilizes the principle of superposition of simple sources, was used in this study. This theory models each incremental area of the vibrating plate as a point monopole source near an infinitely rigid reflecting surface. The mathematical details of this classical theory are presented here for the

particular case of combined structureborne and airborne inputs.

4.1 DERIVATION OF THE EQUATION FOR THE PRESSURE

Utilizing Huygens principle of superposition of simple sources the sound generation of each incremental area, dS, of the plate is modeled as a monopole lying on a rigid planar reflecting surface. The incremental pressure in this case is given by (see reference [7])

$$dp(\vec{r}',t) =$$

$$j\omega\rho_o/(2\pi r')\, e^{-jkr'}\, v(\beta_1,\beta_2,t)\, d\beta_1 d\beta_2 \,. \qquad (35)$$

In the β_i system (see figure 1), the coordinates of the point of observation are $(\beta_1,\beta_2,\beta_3) = (r_1,r_2,r_3)$, and the coordinates of the incremental plate area are $(\beta_1,\beta_2,\beta_3) = (\beta_1,\beta_2,0)$. Thus, the distance from a point in space to the center of the plate is given by

$$r^2 = r_1^2 + r_2^2 + r_3^2, \qquad (36)$$

and the distance from the same point in space to incremental area on the plate which is radiating sound is

$$r'^2 = (r_1-\beta_1)^2 + (r_2-\beta_2)^2 + r_3^2$$

$$= r^2 - 2r_1\beta_1 - 2r_2\beta_2 + \beta_1^2 + \beta_2^2 \ , \qquad (37)$$

where

$$r_1 = r \sin(\theta)\cos(\phi), \qquad (38)$$

$$r_2 = r \sin(\theta)\sin(\phi) \ . \qquad (39)$$

Substituting (38) and (39) into (37)

$$r' = r \left[1 - 2 \sin(\theta)\cos(\phi)(\beta_1/r) - 2 \sin(\theta)\sin(\phi)(\beta_2/r) \right.$$

$$\left. + (\beta_1/r)^2 + (\beta_2/r)^2 \right]^{1/2} \ . \qquad (40)$$

Using the far field approximations

$$r >> d_1 \text{ and } r >> d_2 \qquad (41)$$

$$r' \cong$$

$$r \left[1-\sin(\theta)\cos(\phi)(\beta_1/r)-\sin(\theta)\sin(\phi)(\beta_2/r) \right] \ . \qquad (42)$$

Substituting into equation (35), the expression for the incremental pressure caused by the incremental plate area is

$$dp(\vec{r},t) = j\omega\rho_o/(2\pi r)$$

$$\cdot \ e^{-jkr(1-\sin(\theta)\cos(\phi)(\beta_1/r)-\sin(\theta)\sin(\phi)(\beta_2/r))}$$

$$\cdot \ v(\beta_1,\beta_2,t) \ d\beta_1 d\beta_2 \ . \qquad (43)$$

Integrating over the area of the plate, the pressure at a point in the far acoustic field is given by

$$p(\vec{r},t) = j\omega\rho_o/(2\pi r)\, e^{-jkr}$$

$$\cdot \int_{-d_2/2}^{d_2/2} \int_{-d_1/2}^{d_1/2} \left[e^{jk \sin(\theta)(\beta_1\cos(\phi)+\beta_2\sin(\phi))} \right.$$

$$\left. \cdot\, v(\beta_1,\beta_1,t) \right] d\beta_1 d\beta_1 \,. \qquad (44)$$

Making the following change of variables (see figure 1):

$$\beta_1 = \alpha_1 - d_1/2, \qquad \beta_2 = \alpha_2 - d_2/2 \,. \qquad (45)$$

$$d\beta_1 = d\alpha_1, \qquad d\beta_2 = d\alpha_2 \,, \qquad (46)$$

equation (44) becomes

$$p(\vec{r},t) = j\omega\rho_o/(2\pi r)$$

$$\cdot\, e^{-jk(r + d_1/2 \sin(\theta)\cos(\phi) + d_2/2 \sin(\theta)\sin(\phi))}$$

$$\cdot \int_0^{d_2} \int_0^{d_1} \left[e^{jk \sin(\theta)(\alpha_1\cos(\phi)+\alpha_2\sin(\phi))} \right.$$

$$\left. v(\alpha_1,\alpha_2,t) \right] d\alpha_1 d\alpha_2 \,. \qquad (47)$$

Returning to equation (32) and substituting equation (28) into (32), the velocity of the plate can be shown to be

$$v(\alpha_1,\alpha_2,t) = j\omega\, e^{j\omega t}$$

$$\cdot \sum_{m=1}^{\infty} \sum_{n=1}^{\infty} \eta_{mn}\, e^{-j\theta_{mn}} \sin(m\pi\alpha_1/d_1)\sin(n\pi\alpha_2/d_2) \; . \qquad (48)$$

Substituting equation (48) into equation (47)

$$p(\vec{r},t) = -\omega^2\rho_o/(2\pi r)$$

$$\cdot\, e^{j(\omega t - k(r + d_1/2\, \sin(\theta)\cos(\phi) + d_2/2\, \sin(\theta)\sin(\phi)))}$$

$$\cdot \sum_{m=1}^{\infty} \sum_{n=1}^{\infty} \Bigg[\eta_{mn}\, e^{-j\theta_{mn}}$$

$$\cdot \int_0^{d_1} e^{jk\, \sin(\theta)\cos(\phi)\, \alpha_1} \sin(m\pi\alpha_1/d_1)\, d\alpha_1$$

$$\cdot \int_0^{d_2} e^{jk\, \sin(\theta)\sin(\phi)\, \alpha_2} \sin(n\pi\alpha_2/d_2)\, d\alpha_2 \Bigg] \; . \qquad (49)$$

4.2 EVALUATION OF THE INTEGRALS

The integrals in equation (49) can be written as

$$Z_m = \int_0^{d_1} e^{jk \sin(\theta)\cos(\phi)\ \alpha_1} \sin(m\pi\alpha_1/d_1)\ d\alpha_1$$

$$= \int_0^{d_1} \cos(k \sin(\theta)\cos(\phi)\ \alpha_1) \sin(m\pi\alpha_1/d_1)\ d\alpha_1$$

$$+ j \int_0^{d_1} \sin(k \sin(\theta)\cos(\phi)\ \alpha_1) \sin(m\pi\alpha_1/d_1)\ d\alpha_1 \ . \qquad (50)$$

and

$$Z_n = \int_0^{d_2} e^{jk \sin(\theta)\sin(\phi)\ \alpha_2} \sin(n\pi\alpha_2/d_2)\ d\alpha_2$$

$$= \int_0^{d_2} \cos(k \sin(\theta)\sin(\phi)\ \alpha_2) \sin(n\pi\alpha_2/d_2)\ d\alpha_2$$

$$+ j \int_0^{d_2} \sin(k \sin(\theta)\sin(\phi)\ \alpha_2) \sin(n\pi\alpha_2/d_2)\ d\alpha_2 \ . \qquad (51)$$

With the integrals represented in this form, they can be evaluated by making a trigonometric substitution followed by straightforward integration, or more simply by looking them up in tables of integrals.

4.3 CALCULATION OF THE SOUND POWER RADIATED

With the integrals of equation (49) evaluated as discussed in the previous section, the equation for pressure can be written as:

$$p(\vec{r},t) = -\omega^2\rho_o/(2\pi r)$$

$$\cdot\, e^{j(\omega t - k(r + d_1/2\, \sin(\theta)\cos(\phi) + d_2/2\, \sin(\theta)\sin(\phi)))}$$

$$\cdot \sum_{m=1}^{\infty} \sum_{n=1}^{\infty} \left[\eta_{mn}\, e^{-j\theta_{mn}}\, Z_m\, Z_n \right] . \qquad (52)$$

From this last equation, the acoustic pressure at an arbitrary point in space can be calculated where it has been assumed that the point of observation is in the far acoustic field, i.e. $r >> d_1$ and $r >> d_2$. The time averaged magnitude of the acoustic intensity vector in the radially outward direction at a far-field point in space for a simple harmonic, monopole source is given by

$$\langle I_{r'}(\vec{r}',t)\rangle_t = |p(\vec{r}',t)|^2/(2\rho_o c_o) . \qquad (53)$$

This relationship also holds for the simply supported rectangular plate when $r >> d_1$ and $r >> d_2$. Making the appropriate substitutions, the far field time averaged magnitude of the acoustic intensity vector in the radially outward direction at a point in space for the plate vibrating in simple harmonic motion is given by

$$<I_r(\vec{r},t)>_t = p^*(\vec{r},t)p(\vec{r},t)/(2\rho_o c_o)$$

$$= (\rho_o \omega^2/(2\pi r))^2/(2\rho_o c_o)$$

$$\cdot \left[\sum_{k=1}^{\infty} \sum_{l=1}^{\infty} \eta_{kl} \, e^{+j\theta_{kl}} \, z_k^* \, z_l^* \right]$$

$$\cdot \left[\sum_{m=1}^{\infty} \sum_{n=1}^{\infty} \eta_{mn} \, e^{-j\theta_{mn}} \, z_m \, z_n \right] . \qquad (54)$$

Rearranging the order of summation

$$<I_r(\vec{r},t)>_t = (\rho_o \omega^2/(2\pi r))^2/(2\rho_o c_o) \sum_{k=1}^{\infty} \sum_{l=1}^{\infty} \sum_{m=1}^{\infty} \sum_{n=1}^{\infty}$$

$$\left[\eta_{kl} \, e^{+j\theta_{kl}} \, \eta_{mn} \, e^{-j\theta_{mn}} \, z_k^* \, z_l^* \, z_m \, z_n \right] . \qquad (55)$$

The time averaged sound power is given by

$$<\Pi(t)>_t = \int \int <\vec{I} \cdot \vec{n}>_t \, dS . \qquad (56)$$

In the present case, the surface to be integrated over is a hemisphere in the far acoustic field, and the normal unit vector is in the radially outward direction. Thus

$$\langle \Pi(t) \rangle_t = \int_0^{2\pi} \int_0^{\pi/2} \langle I_r(t) \rangle_t \, r^2 \sin(\theta) \quad d\theta d\phi \, . \tag{57}$$

The time averaged sound power radiated by the plate is therefore given by

$$\langle \Pi(t) \rangle_t =$$

$$\int_0^{2\pi} \int_0^{\pi/2} \left[(\rho_o \omega^2/(2\pi))^2 \sin(\theta)/(2\rho_o c_o) \sum_{k=1}^{\infty} \sum_{l=1}^{\infty} \sum_{m=1}^{\infty} \sum_{n=1}^{\infty} \right.$$

$$\left. \left[\eta_{kl} \, e^{+j\theta_{kl}} \, \eta_{mn} \, e^{-j\theta_{mn}} \, Z_k^* \, Z_l^* \, Z_m \, Z_n \right] \right] d\theta d\phi \, . \tag{58}$$

From equation (28) it can be shown that

$$\eta_{kl} \, e^{+j\theta_{kl}} \, \eta_{mn} \, e^{-j\theta_{mn}} = e^{j(\gamma_{kl} - \gamma_{mn})} \cdot \left[s_{kl} \, s_{mn} + a_{kl} \, a_{mn} \right.$$

$$\left. + \, s_{kl} \, a_{mn} \, e^{j(\phi_s - \phi_a)} + a_{kl} \, s_{mn} \, e^{j(\phi_a - \phi_s)} \right]. \tag{59}$$

Substituting equation (59) into equation (58) the result is

$$\langle \Pi(t) \rangle_t =$$

$$\int_0^{2\pi} \int_0^{\pi/2} \left[(\rho_o \omega^2/(2\pi))^2 \sin(\Theta)/(2\rho_o c_o) \sum_{k=1}^{\infty} \sum_{l=1}^{\infty} \sum_{m=1}^{\infty} \sum_{n=1}^{\infty} \right.$$

$$\left[s_{kl}\, s_{mn} + a_{kl}\, a_{mn} + s_{kl}\, a_{mn}\, e^{j(\phi_s - \phi_a)} + a_{kl}\, s_{mn}\, e^{j(\phi_a - \phi_s)} \right]$$

$$\left. \cdot\, e^{j(\gamma_{kl} - \gamma_{mn})}\, Z_k^*\, Z_l^*\, Z_m\, Z_n \right] d\Theta d\phi \,. \qquad (60)$$

Since the sound power is a real quantity, the series in equation (60) must be real. Using simple complex algebra, the equation for sound power can be written as:

$$<\Pi(t)>_t =$$

$$\int_0^{2\pi}\int_0^{\pi/2} (\rho_o\omega^2/(2\pi))^2 \sin(\theta)/(2\rho_o c_o) \cdot \Bigg[$$

$$\sum_{k=1}^{\infty}\sum_{l=1}^{\infty}\Bigg[s_{kl}^2 |z_k|^2 |z_l|^2$$

$$+ \mathrm{Re}\Big\{ \sum_{m=1}^{\infty}\sum_{n=1}^{\infty}{}_{(kl\neq mn)} s_{kl}\, s_{mn}\, e^{j(\gamma_{kl}-\gamma_{mn})}\, z_k^*\, z_l^*\, z_m\, z_n \Big\}\Bigg]$$

$$+ \sum_{k=1}^{\infty}\sum_{l=1}^{\infty}\Bigg[a_{kl}^2 |z_k|^2 |z_l|^2$$

$$+ \mathrm{Re}\Big\{ \sum_{m=1}^{\infty}\sum_{n=1}^{\infty}{}_{(kl\neq mn)} a_{kl}\, a_{mn}\, e^{j(\gamma_{kl}-\gamma_{mn})}\, z_k^*\, z_l^*\, z_m\, z_n \Big\}\Bigg]$$

$$+ \sum_{k=1}^{\infty}\sum_{l=1}^{\infty} 2\Bigg[s_{kl}\, a_{kl} \cos(\phi_s-\phi_a) |z_k|^2 |z_l|^2$$

$$+ \mathrm{Re}\Big\{ \sum_{m=1}^{\infty}\sum_{n=1}^{\infty}{}_{(kl\neq mn)} s_{kl}\, a_{mn}\, e^{j(\phi_s-\phi_a)}\, e^{j(\gamma_{kl}-\gamma_{mn})}$$

$$\cdot z_k^*\, z_l^*\, z_m\, z_n \Big\}\Bigg]\Bigg] \, d\theta d\phi \, . \qquad (61)$$

The last term in equation (61) accounts for the interaction between the structureborne and airborne inputs in terms of the sound power radiated. Thus, equation (61) similarly shows that the sound power generated by the panel due to the combined airborne and structureborne inputs is, in general, not equal to the to the sum of the individual sound powers

radiated by the panel due to the airborne and structureborne inputs acting individually. Unlike equation (34) for the panel dynamics, however, equation (61) contains cross terms between the different modes of the structure. The additional cross terms between different flexural modeshapes arise because the spatial average of the acoustic intensity used in calculating the sound power takes place over a hemispherical surface in the far acoustic field, and not over the surface of the plate (the area of spatial averaging for the analysis of the dynamic response of the plate). Thus, the orthogonality principle does not apply when calculating the sound power radiated by the plate. Furthermore, equation (61) indicates that even when the structureborne and airborne inputs are precisely 90 degrees out of phase (uncorrelated), there are still many non-zero cross term components between the two inputs which contribute to the total sound power radiated due to the existence of the cross terms between different flexural modes of the structure. Therefore, in general, the total sound power radiated due to the simultaneously combined structureborne and airborne inputs is never exactly equal to the sum of the sound powers radiated due to the structureborne and airborne inputs acting individually.

5. RESULTS

This section contains selected results of a numerical implementation of the analytical model. Source code listings of the computer programs used in the analytical studies are given in reference [5]. The analytical results shown here are intended to simulate the noise radiation of a .8 mm (0.032 inch) thick plate constructed of AA 2024 aluminum (surface density of 2.22 kg/m^2) due to both the individual and combined acoustic and vibrational inputs. The physical dimensions of the plates were chosen to be 0.406 m x 0.241 m (16 in x 9.5 in) since an extensive study of the transmission loss properties of plates of this size had already been completed by NASA researchers. Unless explicitly stated otherwise, the results are for the case of a normally incident, spatially uniform, 1 Pa peak acoustic load and a 0.01 N peak point vibrational load located at the coordinates of α_1= 0.060 m and α_2= 0.135 m. Also, unless stated otherwise, the small damping model (equation (18)) was used in the simulations. In all cases the forcing functions were applied uniformly over the frequency range at 2 Hz intervals.

The results that follow are divided into three sections. In the first section, the effects of the relative magnitudes and phase of the inputs are investigated. In second section, the effects produced by changing the shaker

location (altering the path of the structureborne input) are examined. Finally, the third section examines the effects of adding damping treatment to the aluminum plate.

5.1 EFFECTS OF RELATIVE MAGNITUDE AND PHASE

5.1.1 Analytical Results for a Dominant Airborne Source

Figure (2) shows the sound power levels produced by the individual airborne and structureborne inputs. This figure shows that, in this case, the airborne source is dominant.

The sound powers produced by combining the airborne and structureborne inputs with phase angle differences of 90 degrees, 0 degrees, and 180 degrees are shown in figures (3), (4), and (5) respectively. Figure (3) shows that the sum of the results of the individual inputs is roughly equivalent to results obtained by combining the inputs at 90 degrees over most of the frequency range. Figure (3) also shows that, at least in some isolated frequency regions, there can be a considerable difference between the sum of the individual sound power components and the combined sound power of the uncorrelated inputs. Examination of equation (61) leads one to the conclusion that the differences in the two curves of figure (3) can only be caused by cross terms between the inputs that represent cross coupling between different modes of the structure. Figures (4) and (5) show that even larger deviations between sound powers produced by the sum of the individual inputs and the combined inputs

occur when the inputs are combined at 0 or 180 degrees. These results underscore the importance of the cross terms contained in equation (61) by showing that their contribution to the overall sound power radiated can be as large as the dominant term. Furthermore, since the sign of the cross terms can be positive or negative, the overall noise generated can vary over a very large range depending on the relative phase of the inputs.

5.1.2 Analytical Results for a Dominant Structureborne Source

Figure (6) shows the computed sound power levels produced by the aluminum plate due to a 0.2 Pa peak acoustic load and an independent 0.05 N peak vibrational load. This figure shows that, in this case, the structureborne source is dominant.

The sound powers produced by combining these two inputs with phase angles of 90 degrees, 0 degrees, and 180 degrees are shown in figures (7), (8), and (9) respectively. Particularly good agreement between the sum of the individual inputs and the case of uncorrelated, combined inputs is seen to occur in figure (7). This is an indication that the cross coupling between different modes of the structure play a relatively minor role in this case. Figures (8) and (9) again shows that large deviations between the cases of the sum of the individual inputs and the combined inputs occur

when the inputs are combined at 0 or 180 degrees. Thus, the cross terms between the inputs for like modes can still be responsible for a significant portion of the overall sound radiation in this case.

5.2 EFFECTS OF ALTERING THE INPUT PATHS (SHAKER LOCATION)

5.2.1 Analytical Results for a Dominant Airborne Source

Figures (10) through (13) show the results that were obtained from the analytical programming for the case of a normally incident uniform acoustic load and a point vibrational load located at the new coordinates of $\alpha_1 = 0.121$ m and $\alpha_2 = 0.203$ m. These coordinates place the vibrational point load at the center of the plate, thus driving the same modes as the acoustic input (i.e. the odd modes of the plate).

Figure (10) shows the sound power levels produced by the aluminum plate due to a 1 Pa peak acoustic load and an independent 0.01 N peak vibrational load. This figure shows that the airborne source is dominant or at least of equal influence over the entire frequency range for these inputs.

The sound powers produced by combining the two inputs are shown in figures (11) through (13). These figures show that the overall noise radiation due to combined inputs is extremely sensitive to changes in the relative phases between the inputs. This result indicates that the cross terms have an even larger influence on the overall noise

radiation if and when the airborne and structureborne inputs drive the same modes of the structure.

5.3 EFFECTS OF ADDED DAMPING

5.3.1 Analytical Results for a Dominant Airborne Source

Figures (14) through (17) show the results that were obtained from the analytical program for baseline conditions (shaker located at α_1= 0.060 m and α_2= 0.135 m) on the aluminum plate using the more moderate level of damping included in the model (equation (12)).

Figure (14) shows the sound power levels produced by the aluminum plate due to a 1 Pa peak acoustic load and an independent 0.01 N peak vibrational load. This figure shows that the airborne source is highly dominant over the entire frequency range.

The sound powers produced by combining these two inputs are shown in figures (15) through (17). The sound power curves of figure (15) suggest that cross coupling between different modes occurs in the same frequency regions as figure (3) (the case of small damping). Figures (16) and (17) show that the overall noise radiation due to combined inputs is again very sensitive to changes in the relative phases between the inputs. The figures show that the sound power level can vary as much as 5 dB in isolated frequency regions due to the influence of the cross terms. The increased smoothness of the sound power curves, due to the

added damping, makes the effects of the cross terms particularly evident.

6. DISCUSSION AND CONCLUSIONS

To the author's knowledge, this is the first analytical study of the problem of the sound radiation of aircraft type materials due to fully coherent combined airborne and structureborne inputs in the low frequency regime. The single most significant finding in the results of this study was the discovery of the relative importance of the cross term sound power components. The importance of this finding can not be over emphasized in light of the fact that all of the previous analytical and experimental studies performed in the last 7 or 8 years have neglected the interaction between the airborne and structureborne inputs in the low frequency regime. In a recent review paper (see reference [1]) it was found that 93 publications appeared in the open literature between 1978 and 1984 which devoted their attention strictly to the airborne noise transmission through the sidewalls of aircraft. A smaller number of studies (see references [2]-[4]), addressing the problem of structureborne noise paths in aircraft, similarly restricted the scope of their analysis. As a result of this study, some of the conclusions of these earlier studies regarding the effectiveness of certain noise control treatments may now be in doubt.

Evidence to support this claim can be found in the results such as those found in figures (14) through (17). Computations on the analytical results in these figures (for the damped aluminum panel) show that while the airborne component contributes 82.0 dB overall and the structureborne component contributes 68.6 dB overall, the levels for the combined sound power ranged anywhere from 80.7 dB to 83.3 dB overall. Thus, the overall level of the combined sound power varied over a 2.6 dB range depending on the phase relationship between the airborne and structureborne inputs. Simple calculations show that the sum of individual airborne and structureborne components is 82.2 dB or, in other words, one would expect a 0.2 dB increase in the overall sound power level due to the addition of the structureborne noise to the dominant airborne noise if the sound powers were additive. The implication here is that the structureborne component does not have to radiate a significant amount of noise on its own in order to significantly change the level of the combined sound. In fact, additional results presented in reference [5] indicate that the structureborne component needs only to change the dynamic response of the structure in order to also significantly influence the overall noise radiation.

The results of the study also indicate that the interactive effects are due primarily to cross terms between like

modes of the airborne and structureborne inputs. While the results for uncorrelated inputs showed that the effects of cross coupling between different modes of the structure could be significant in some frequency ranges, the largest interactive effects were found when the airborne and structureborne components were correlated. It should also be noted that, since the cross coupling of different modes enters the problem through the damping model (see equation (61)), the contribution to the sound power due to cross coupling between different modes of the structure may have been a spurious effect that was introduced through the use of equations (18) and (19). Thus, the effects on the combined sound powers due to cross coupling between different modes may or may not be observed experimentally.

REFERENCES

1. J.S. Mixson and C.A. Powell 1984 AIAA/NASA 9th Aeroacoustics Conference, Review of Recent Research on Interior Noise of Propeller Aircraft.

2. V.L. Metcalf and W.H. Mayes 1983 S.A.E. Technical Paper 830735, Structureborne Contribution to Interior Noise of Propeller Aircraft.

3. J.F. Unruh and D.C. Scheidt 1979 S.A.E. Technical Paper Series 790626, Engine Induced Structure-Borne Noise in a General Aviation Aircraft.

4. M.C. Junger et. al. 1984 NASA Contract Report 172381, Analytical Model of the Structureborne Interior Noise Induced by a Propeller Wake.

5. M.C. McGary 1985 Ph.D. Dissertation, Stanford University, Separation of Airborne and Structureborne Noise Radiated by Plates Constructed of Conventional and Composite Materials with Applications for Prediction of Interior Noise Paths in Propeller Driven Aircraft.

6. W. Soedel 1981 Vibrations of Shells and Plates, New York, Marcel Dekker Inc.

7. L.E. Kinsler and A.R. Frey 1962 Fundamentals of Acoustics, New York, John Wiley and Sons Inc.

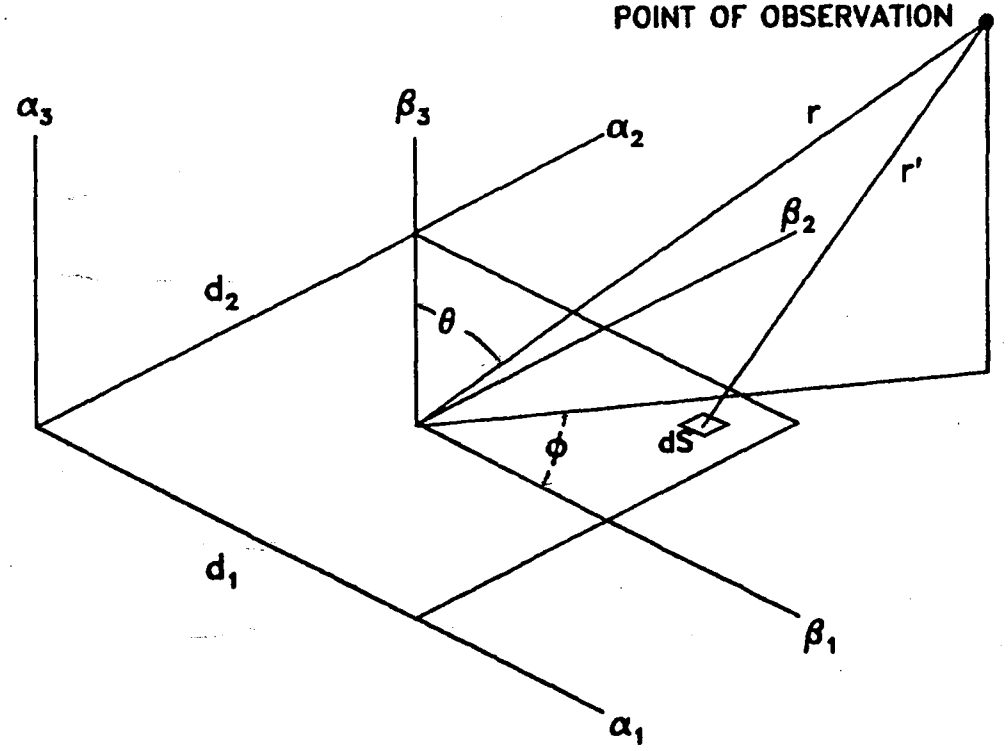

Figure 1 - Geometry of the simply supported plate.

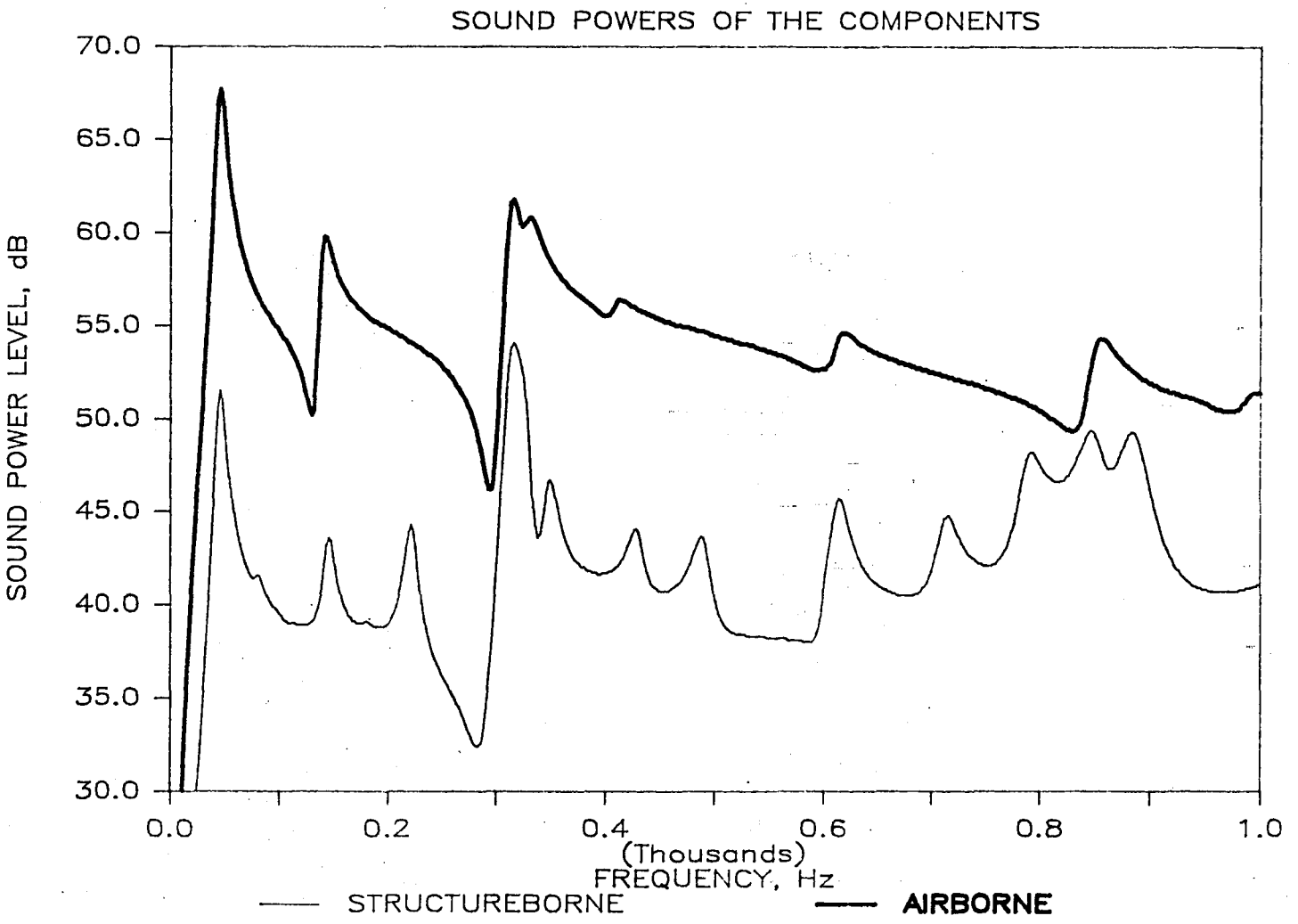

Figure 2 - Predicted sound powers of the individual components for a dominant airborne source and the shaker located near the corner.

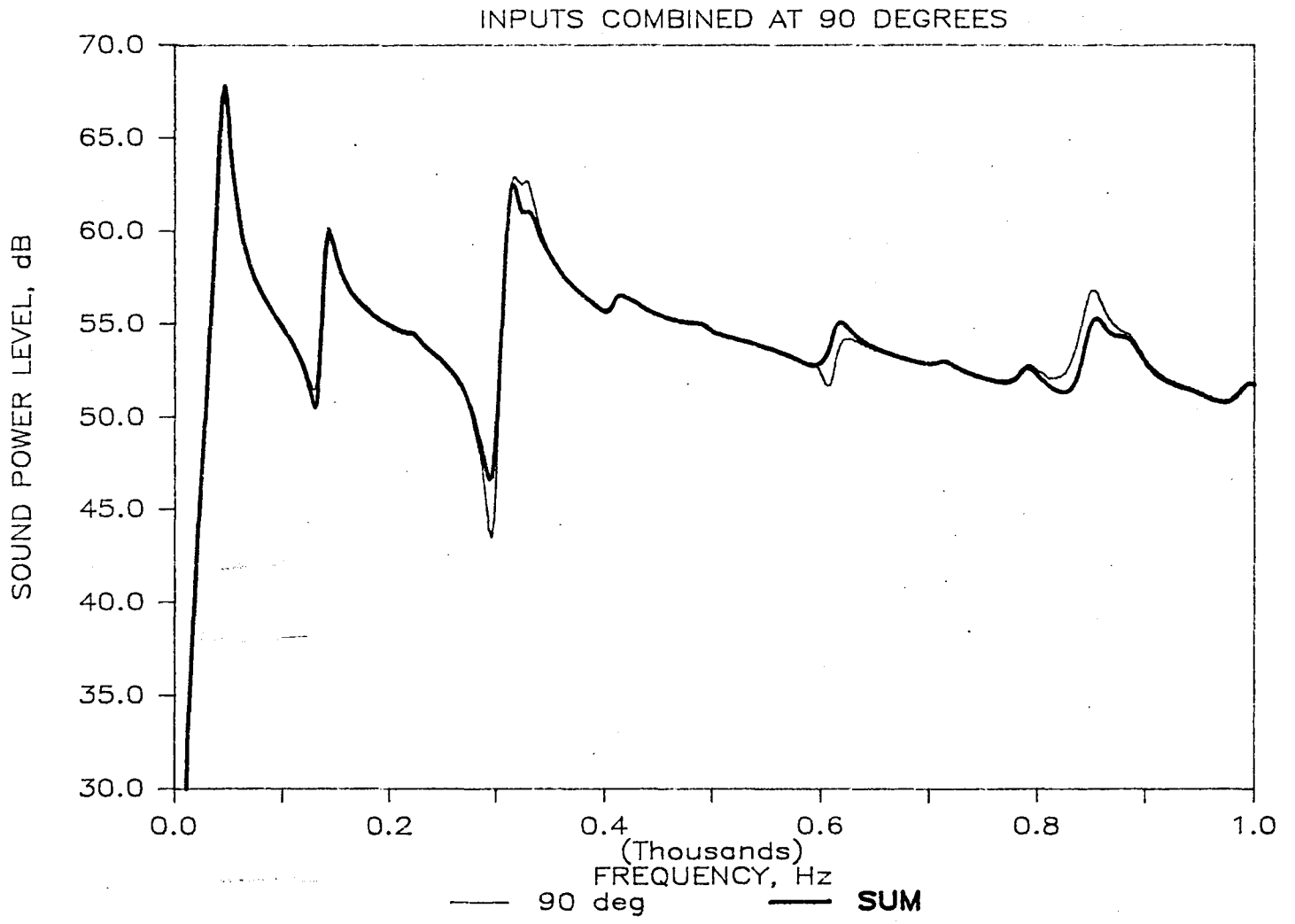

Figure 3 - Predicted sound powers for the case of the inputs combined at 90 degrees with a dominant airborne source and the shaker located near the corner.

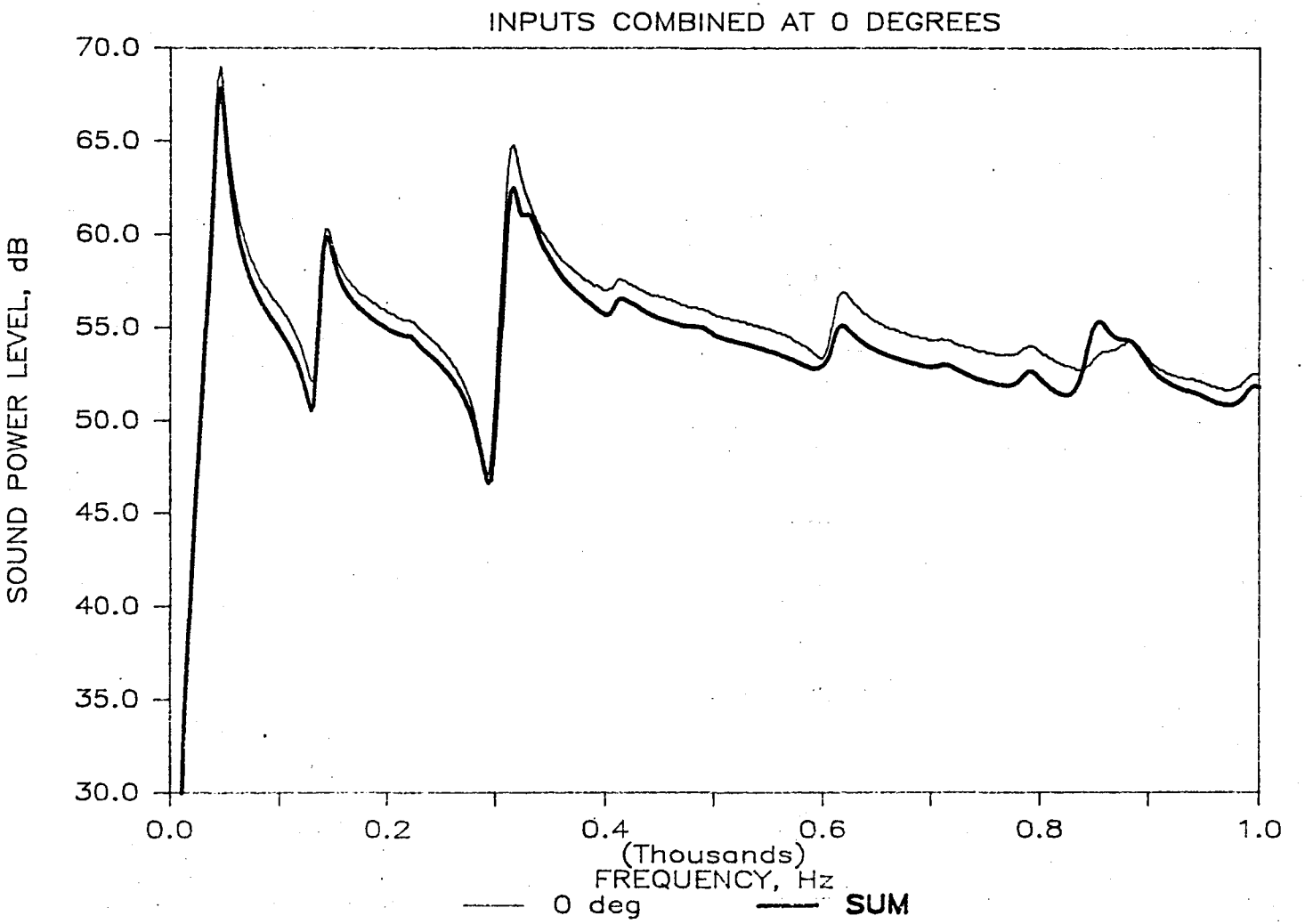

Figure 4 - Predicted sound powers for the case of the inputs combined at 0 degrees with a dominant airborne source and the shaker located near the corner.

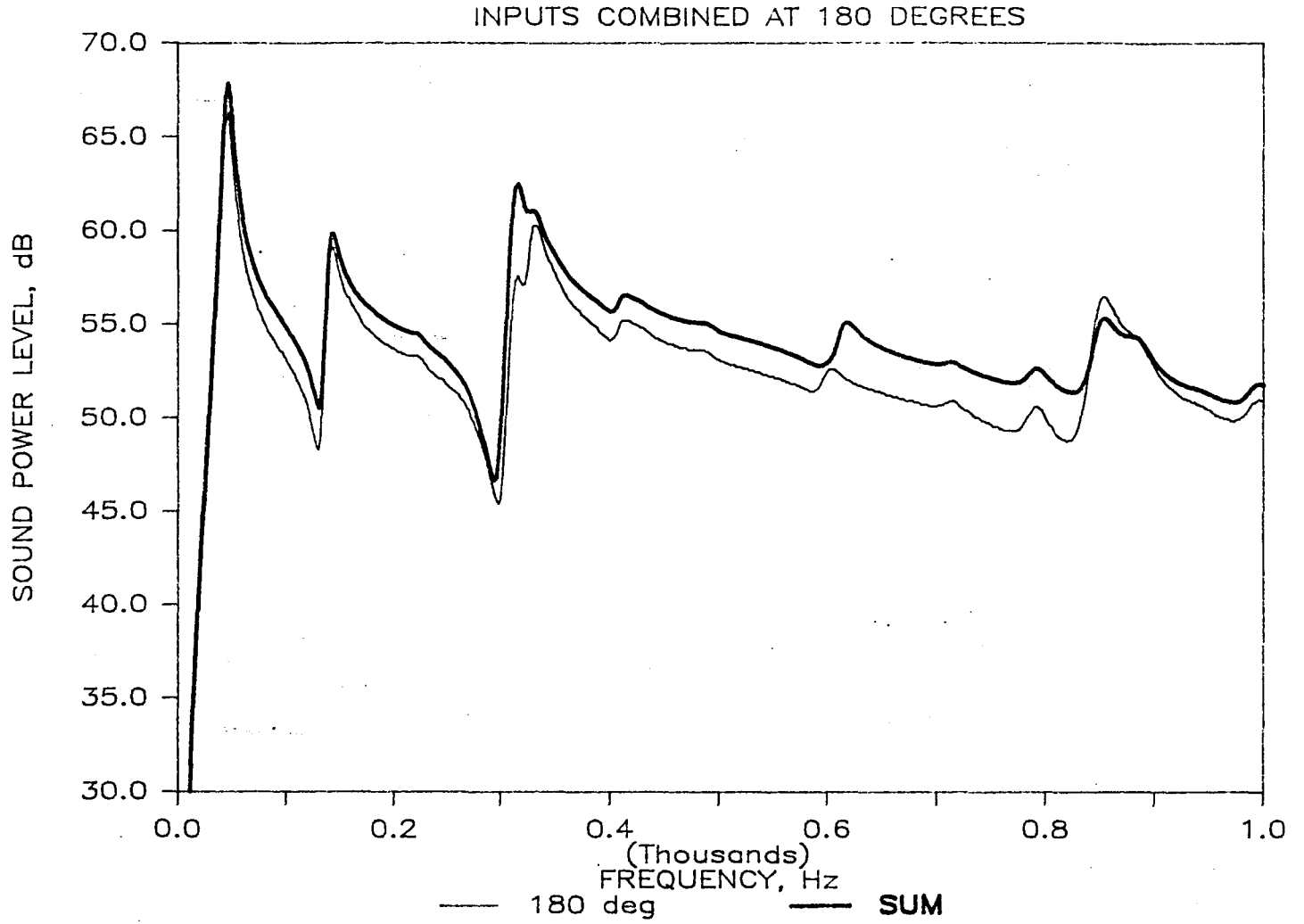

Figure 5 - Predicted sound powers for the case of the inputs combined at 180 degrees with a dominant airborne source and the shaker located near the corner.

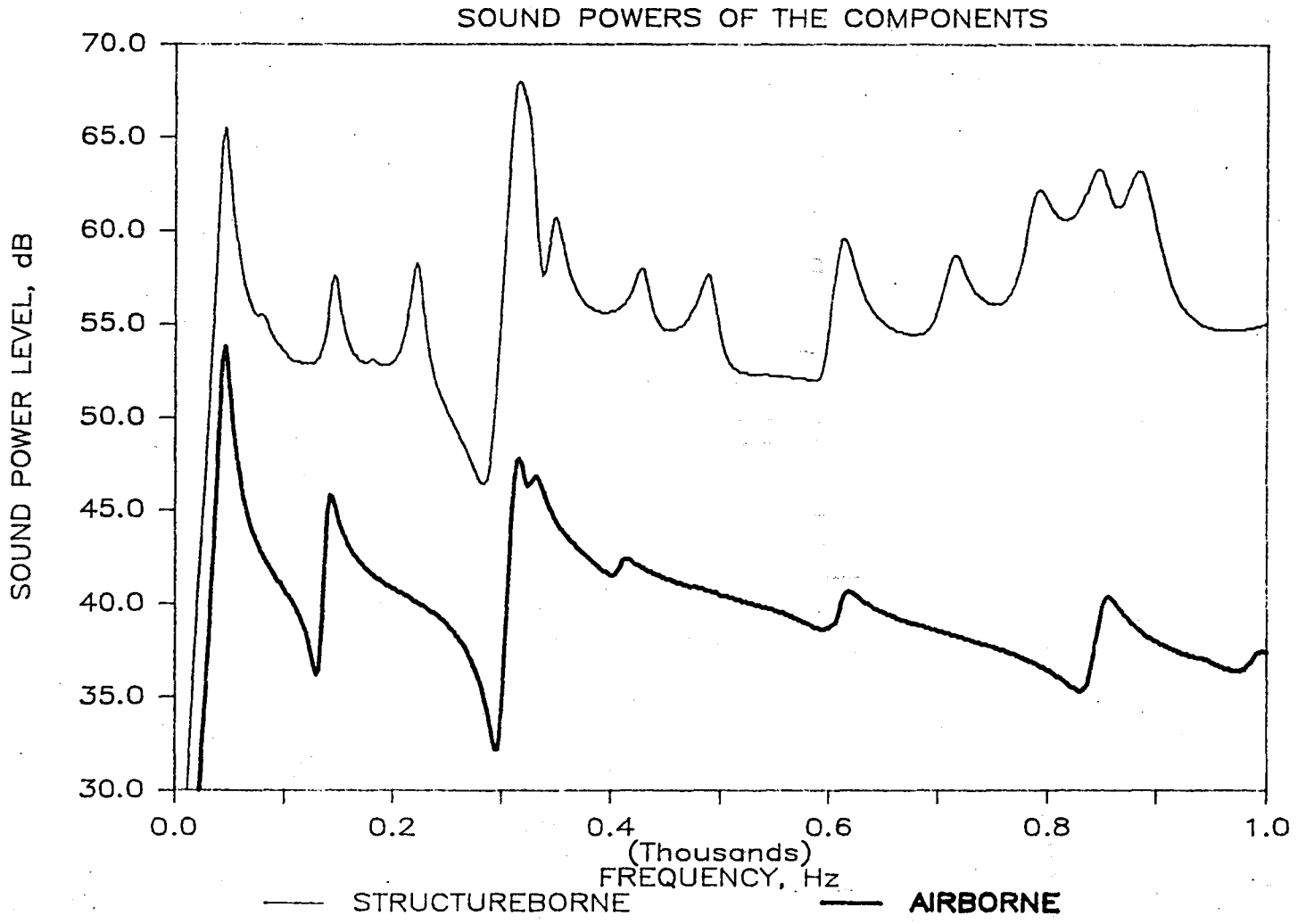

Figure 6 - Predicted sound powers of the individual components for a dominant structureborne source and the shaker located near the corner.

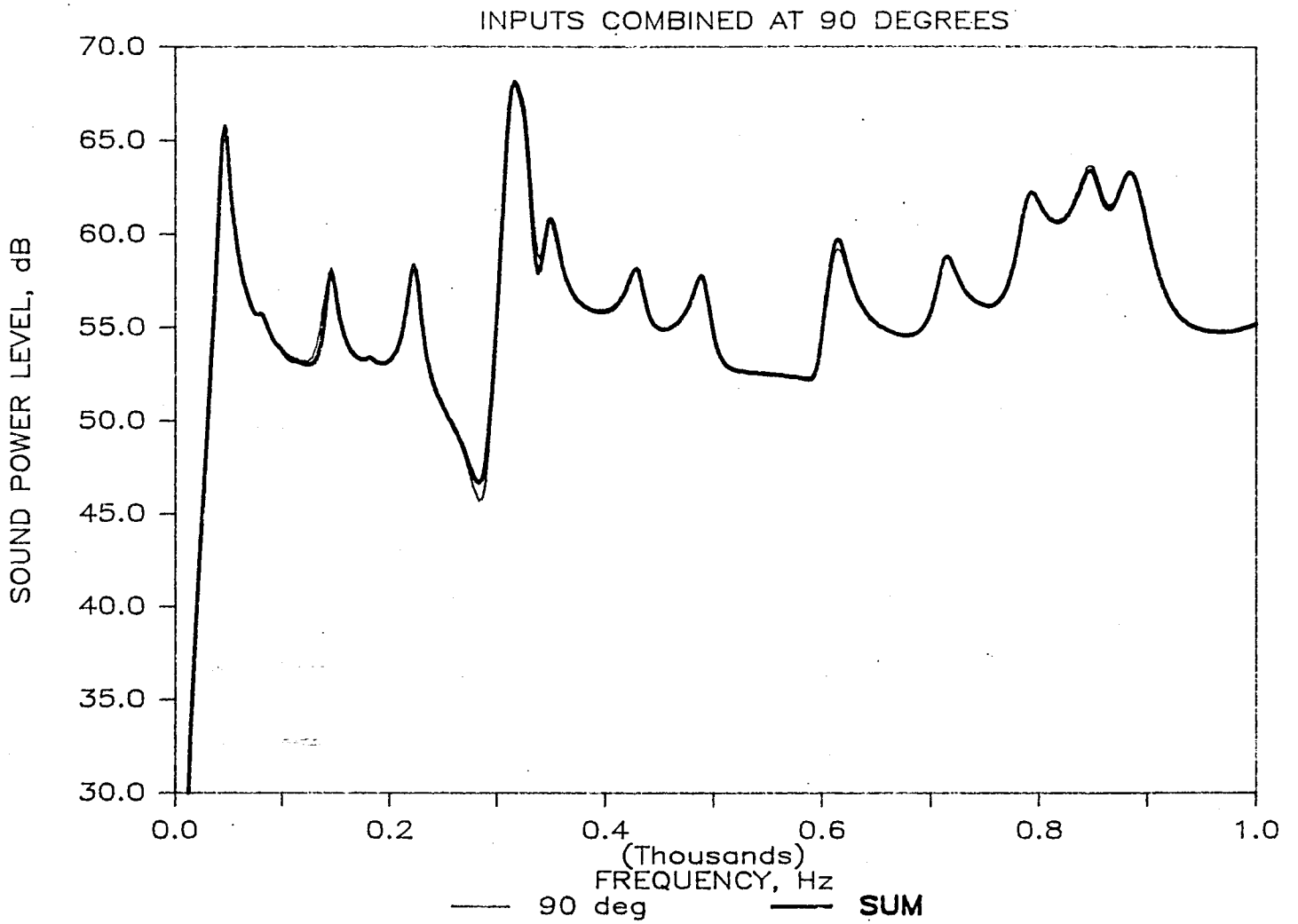

Figure 7 - Predicted sound powers for the case of the inputs combined at 90 degrees with a dominant structureborne source and the shaker located near the corner.

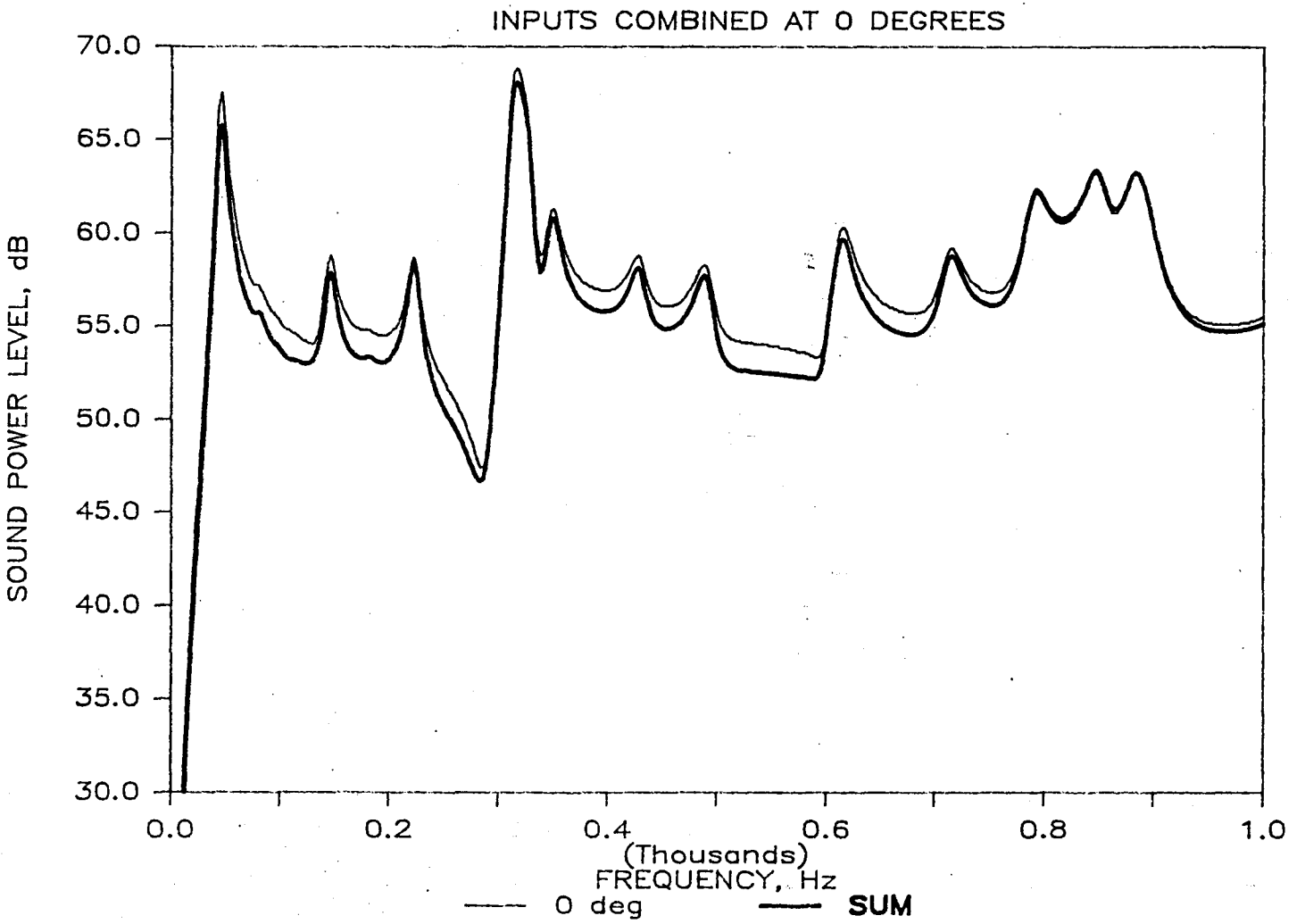

Figure 8 - Predicted sound powers for the case of the inputs combined at 0 degrees with a dominant structureborne source and the shaker located near the corner.

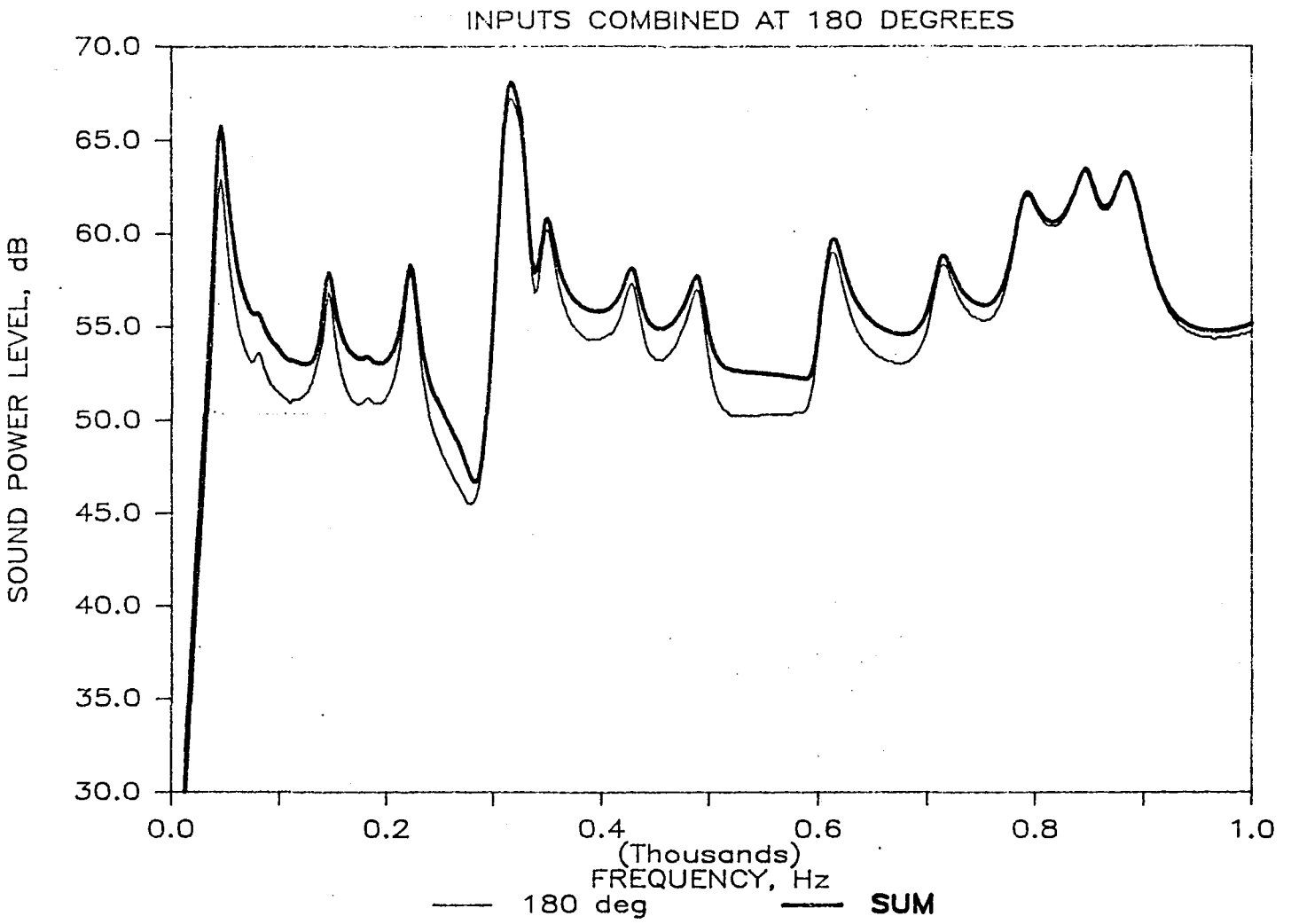

Figure 9 - Predicted sound powers for the case of the inputs combined at 180 degrees with a dominant structureborne source and the shaker located near the corner.

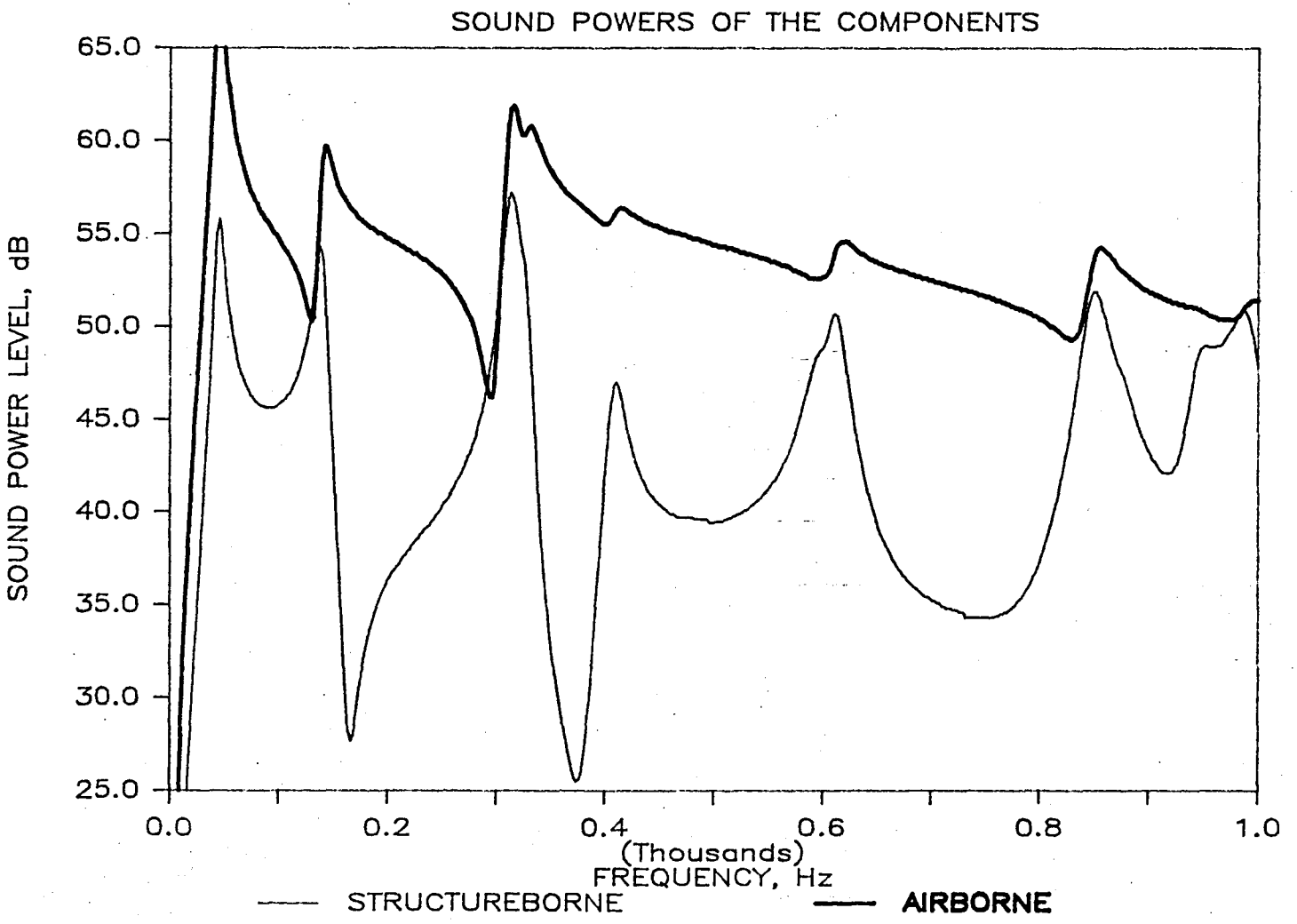

Figure 10 - Predicted sound powers of the individual components for a dominant airborne source and the shaker located at the center.

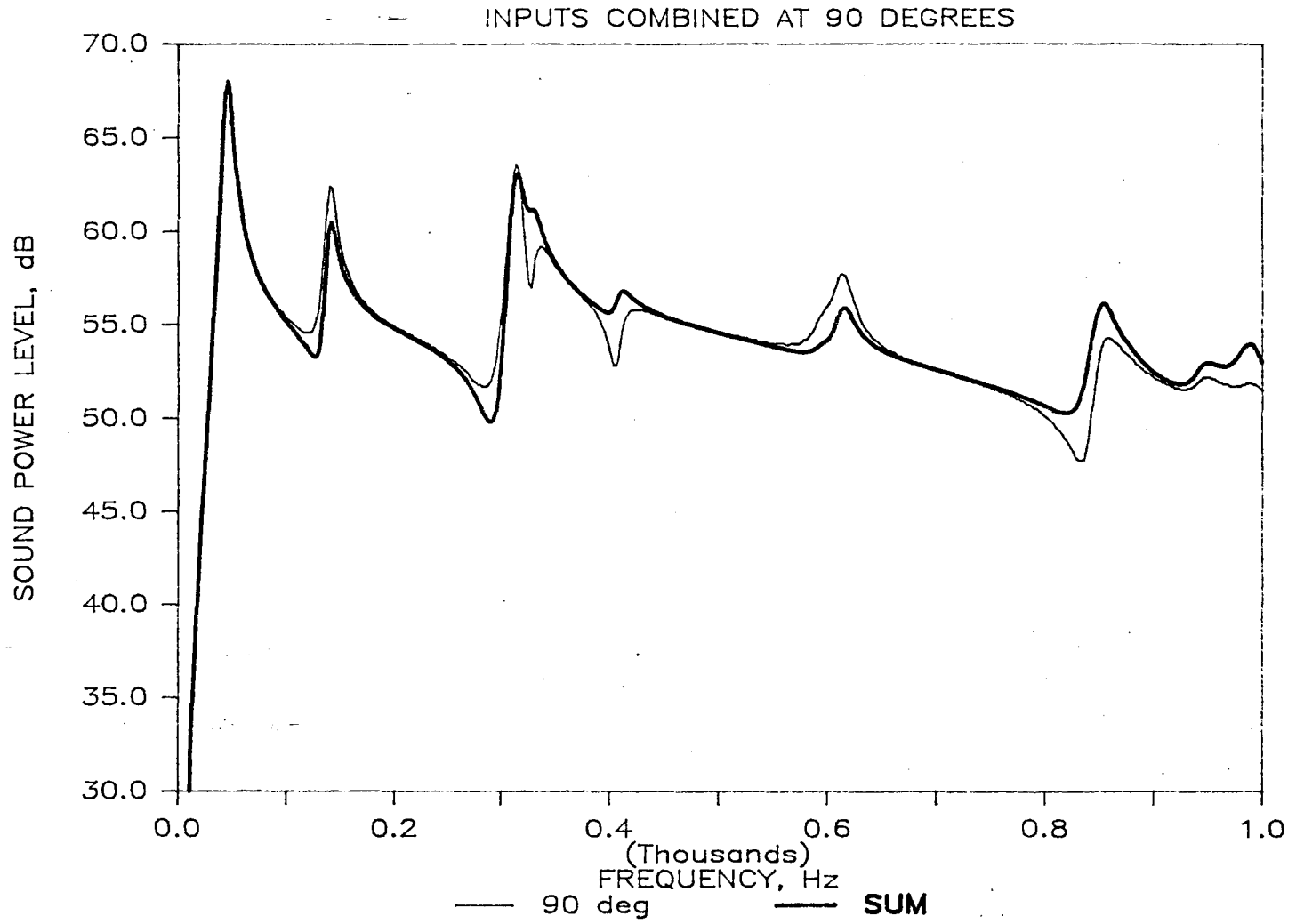

Figure 11 - Predicted sound powers for the case of the inputs combined at 90 degrees with a dominant airborne source and the shaker located at the center.

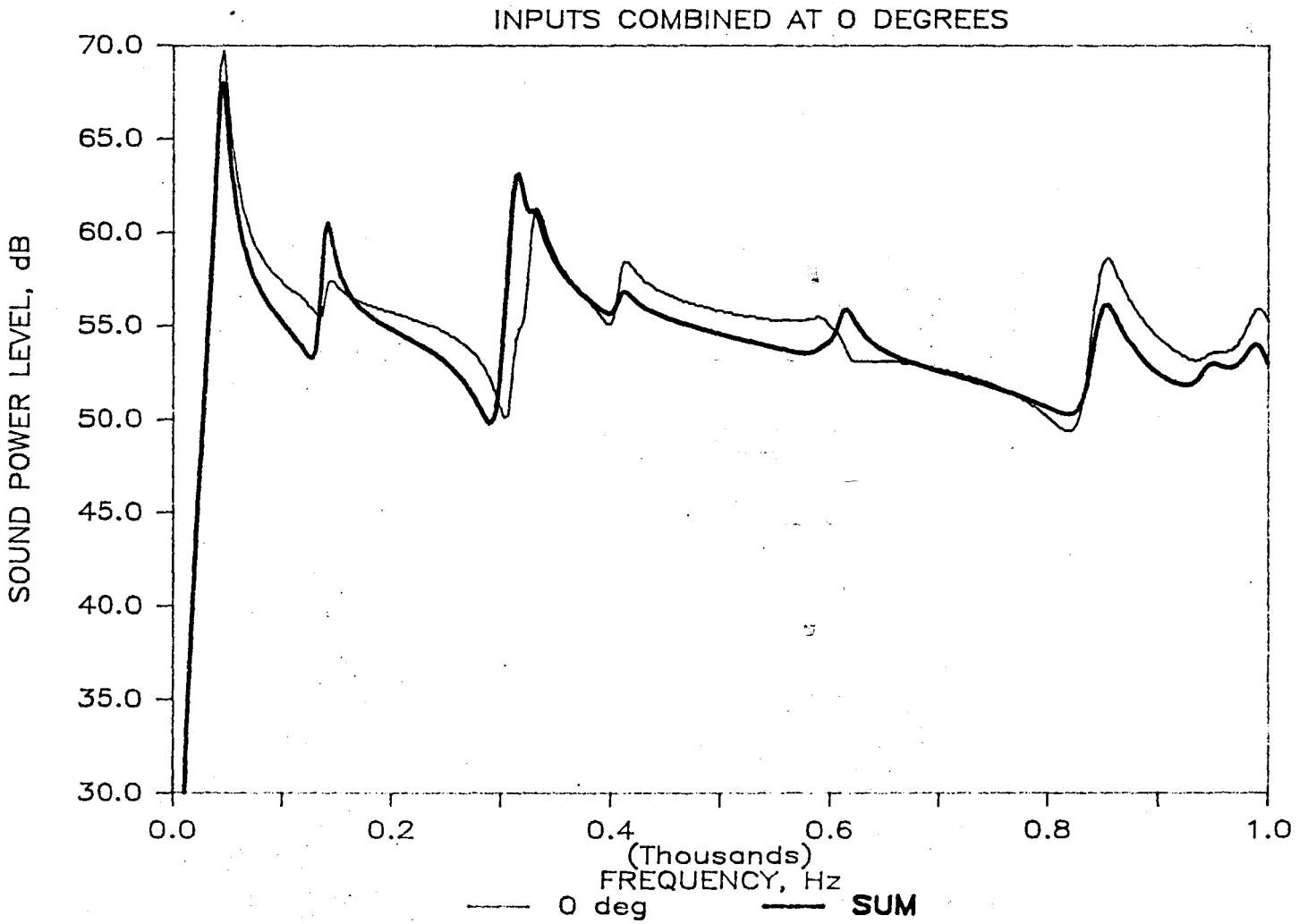

Figure 12 - Predicted sound powers for the case of the inputs combined at 0 degrees with a dominant airborne source and the shaker located at the center.

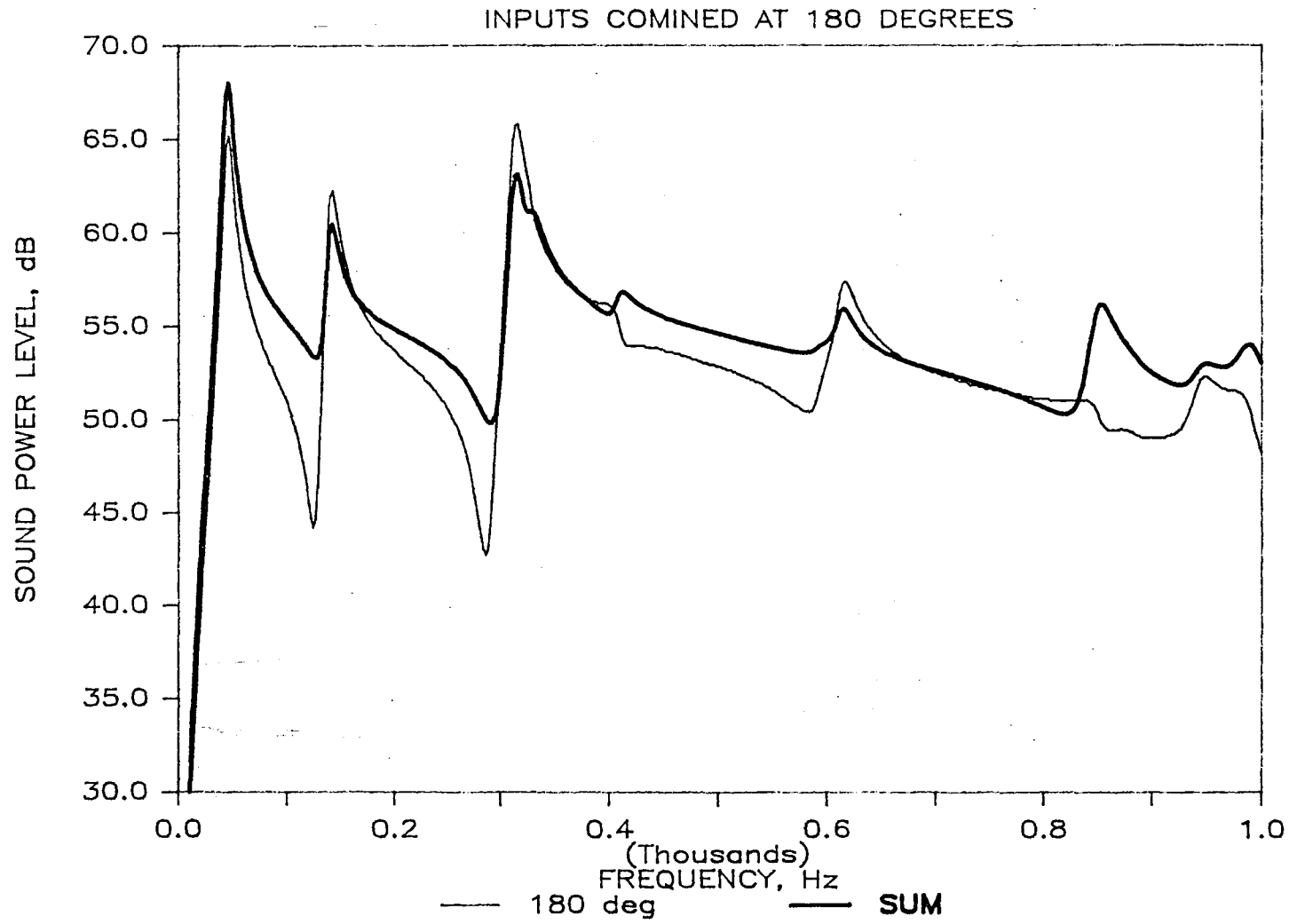

Figure 13 - Predicted sound powers for the case of the inputs combined at 180 degrees with a dominant airborne source and the shaker located at the center.

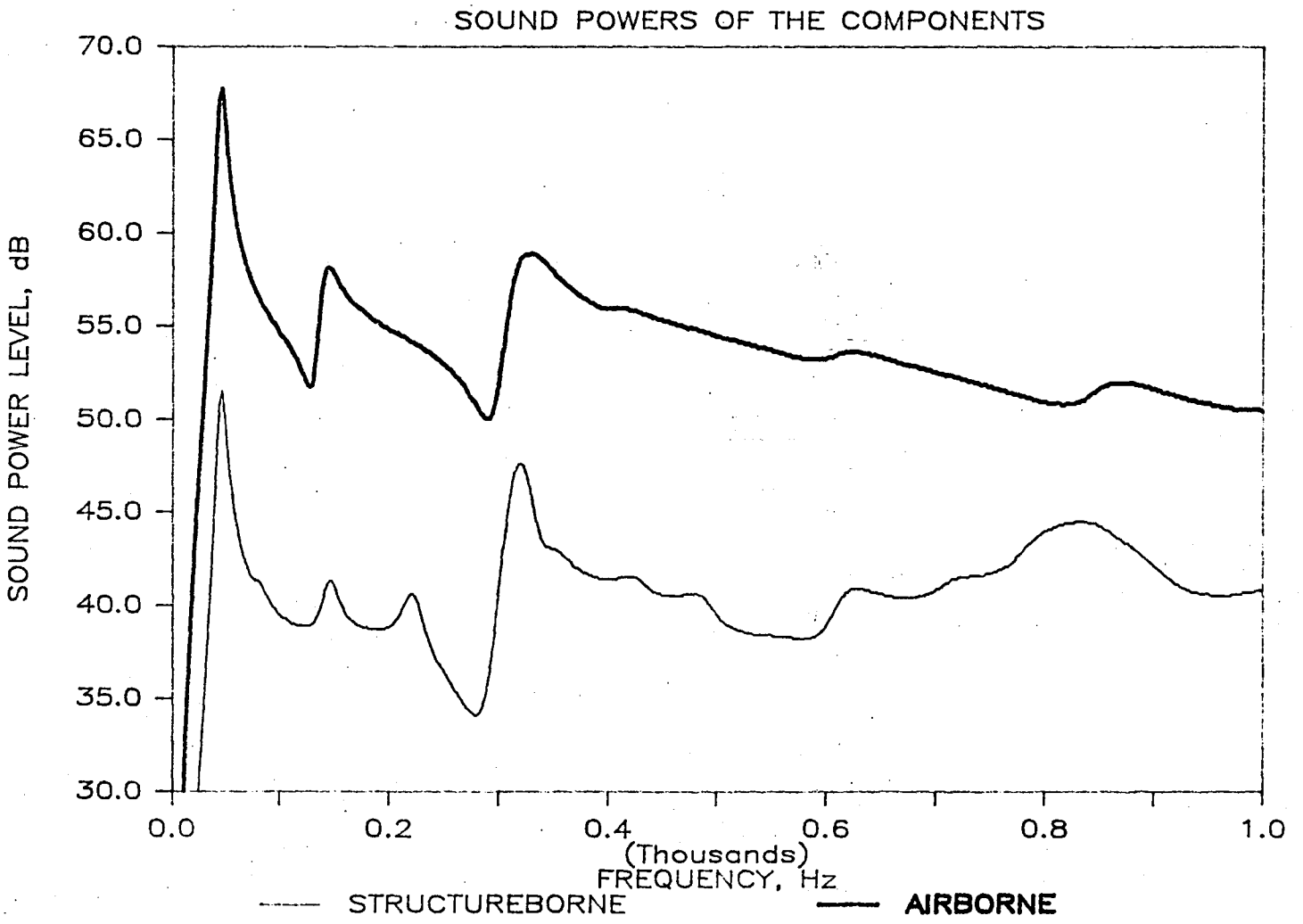

Figure 14 - Predicted sound powers of the individual components for a dominant airborne source, the shaker located near the corner, and a moderate level of damping added to the panel.

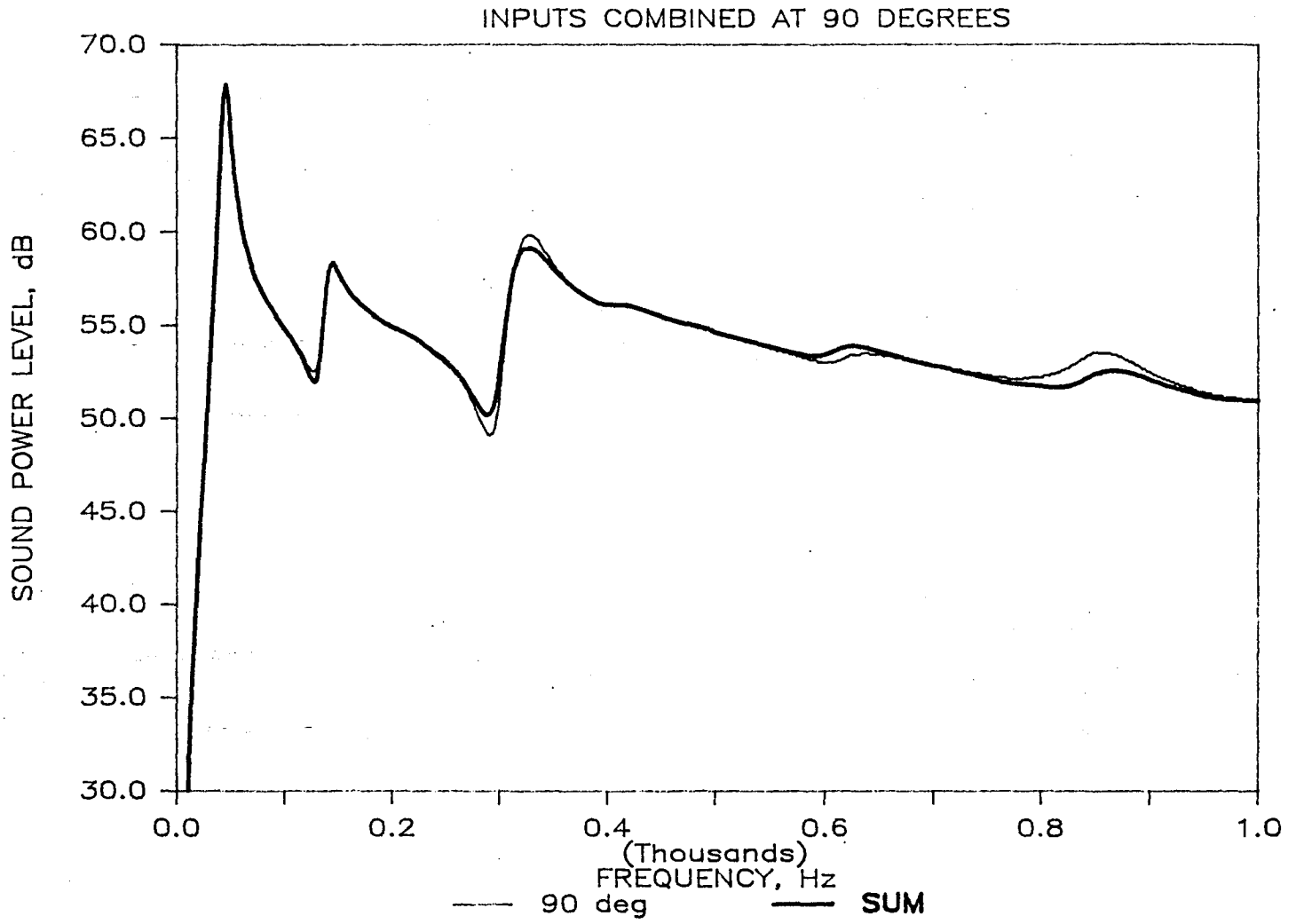

Figure 15 - Predicted sound powers for the case of the inputs combined at 90 degrees with a dominant airborne source, the shaker located near the corner, and a moderate level of damping added to the panel.

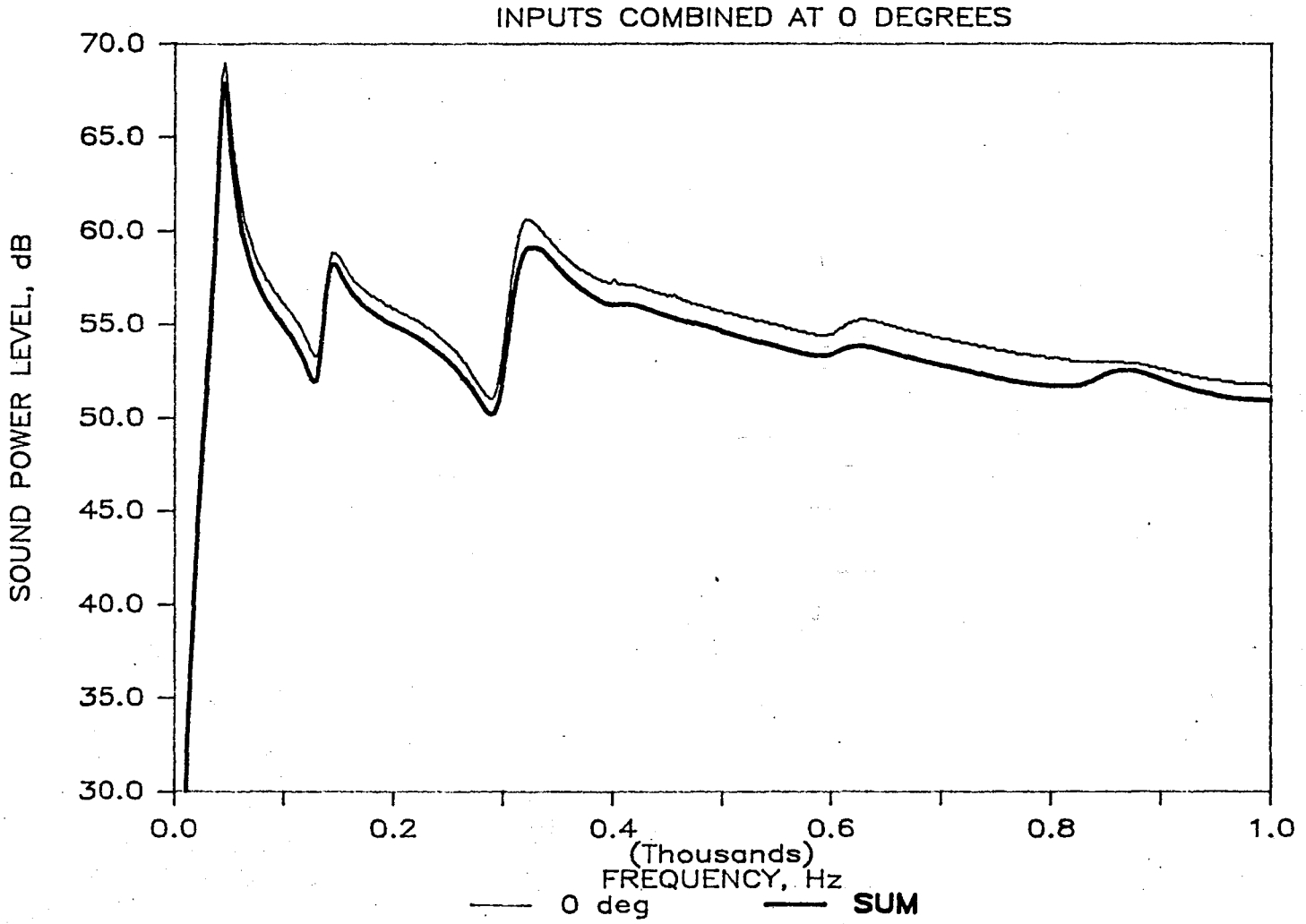

Figure 16 - Predicted sound powers for the case of the inputs combined at 0 degrees with a dominant airborne source, the shaker located near the corner, and a moderate level of damping added to the panel.

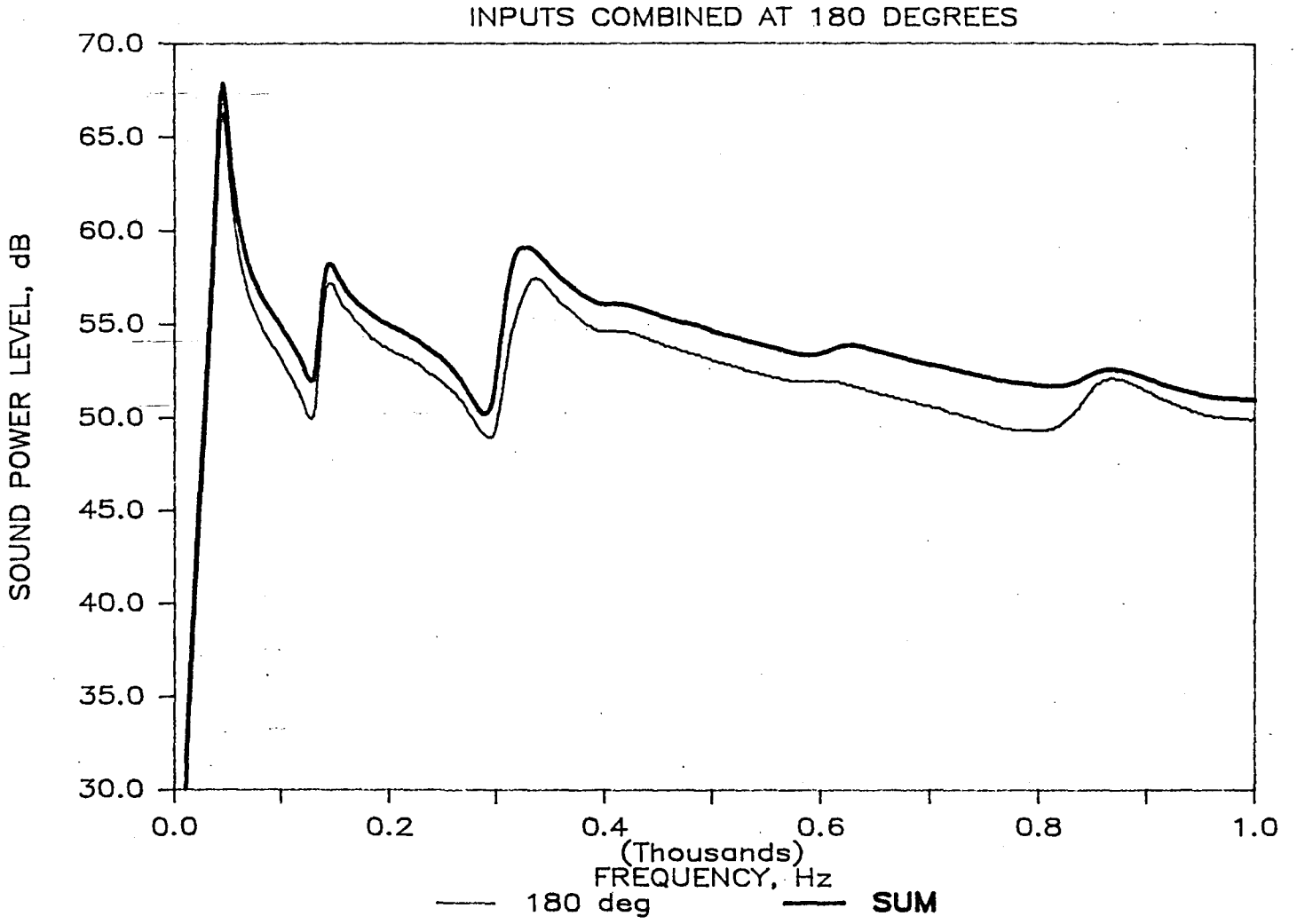

Figure 17 - Predicted sound powers for the case of the inputs combined at 180 degrees with a dominant airborne source, the shaker located near the corner, and a moderate level of damping added to the panel.

1. Report No.	2. Government Accession No.	3. Recipient's Catalog No.
NASA TM-87746		

4. Title and Subtitle	5. Report Date
Interaction of Airborne and Structureborne Noise Radiated by Plates, Volume I - Analytical Study	July 1986
	6. Performing Organization Code: 505-63-11-02
7. Author(s): Michael C. McGary	8. Performing Organization Report No.
	10. Work Unit No.
9. Performing Organization Name and Address: NASA Langley Research Center, Hampton, VA 23665-5225	11. Contract or Grant No.
	13. Type of Report and Period Covered: Technical Memoradum
12. Sponsoring Agency Name and Address: National Aeronautics and Space Administration, Washington, DC 20546	14. Sponsoring Agency Code

15. Supplementary Notes

16. Abstract

An analytical study was undertaken in order to further the understanding of the interaction of airborne and structureborne noise radiated by aircraft materials. The theory and the results of several computer simulations of the noise radiated by thin, isotropic, rectangular aluminum plates due to fully coherent combined acoustic and vibrational inputs is presented. The most significant finding of the study was the extremely large influence that the relative phase between the inputs has on the combined noise radiation of the plates. It is shown that phase dependent effects manifest themselves as cross terms in both the dynamic and acoustic portions of the analysis. The computer simulations show that these cross terms can radically alter the combined sound power radiated by plates constructed of aircraft-type materials. The results of the study suggest that airborne-structureborne interactive effects could be responsible for a significant portion of the overall noise radiated by aircraft-type structures in the low frequency regime. This implies that previous analytical and experimental studies may have neglected an important physical phenomenon in their analyses of the interior noise of propeller driven aircraft.

17. Key Words (Suggested by Author(s))	18. Distribution Statement
Aircraft Interior Noise Acoustic Intensity Airborne Noise Structureborne Noise	Unclassified - Unlimited Subject Category - 71

19. Security Classif. (of this report)	20. Security Classif. (of this page)	21. No. of Pages	22. Price
Unclassified	Unclassified	60	A04

N-305

For sale by the National Technical Information Service, Springfield, Virginia 22161

End of Document